To: Mr. Chas. J. McCarthy
Chance Vaught Corp.

NATIONAL ADVISORY COMMITTEE FOR AERONAUTICS

SPECIAL REPORT No. 101

PRELIMINARY MODEL TESTS OF A WING-DUCT COOLING SYSTEM FOR RADIAL ENGINES

By David Biermann and E. Floyd Valentine
Langley Memorial Aeronautical Laboratory

February 1939

NATIONAL ADVISORY COMMITTEE FOR AERONAUTICS

PRELIMINARY MODEL TESTS OF A WING-DUCT COOLING SYSTEM FOR RADIAL ENGINES

By David Biermann and E. Floyd Valentine

SUMMARY

Wind-tunnel tests were conducted on a model wing-nacelle combination to determine the practicability of cooling radial engines by forcing the cooling air into wing-duct entrances located in the propeller slipstream, passing the air through the engine baffles from rear to front, and ejecting the air through an annular slot near the front of the nacelle. The tests, which were of a preliminary nature, were made on a 5-foot-chord wing and a 20-inch-diameter nacelle. A 3-blade, 4-foot-diameter propeller was used.

The tests indicated that this method of cooling and cowling radial engines is entirely practicable providing the wing of the prospective airplane is sufficiently thick to accommodate efficient entrance ducts. The drag of the cowlings tested was definitely less than for the conventional N.A.C.A. cowling, and the pressure available at low air speed corresponding to operation on the ground and at low flying speeds was apparently sufficient for cooling most present-day radial engines.

INTRODUCTION

The radial engine was developed from considerations of weight, simplicity, and cooling; but the large frontal area has always been a disadvantage. The N.A.C.A. cowling reduced this objection to a negligible amount for many years, but with ever-increasing speeds attention is again focused upon the drag of the engine nacelle. Also, the power output of engines has been increased many times while the projected area has remained substantially constant, which has increased the problem of cooling, particularly on the ground and at low air speeds.

Attention has been drawn recently to the effect of cowlings upon the engine power developed. For many years engineers have suspected that engine-propeller combinations installed in airplanes did not produce the thrust power that was produced when the engines and propellers were tested separately on the stands and in the wind tunnels. Until torque meters were installed on engines for flight measurements, the power loss was generally charged to the propellers; but MacClain and Buck in reference 1 show that the engine does not produce the same power when installed on an airplane that it does on the test stand, due presumably to different temperatures of the various engine parts. With the conventional N.A.C.A. cowling the accessory compartment, which houses the carburetor, supercharger, and manifolds, is filled with relatively hot air; so it would not be surprising if power were lost from this source.

The present cooling-cowling system is intended to be an improvement on the N.A.C.A. cowling from the standpoints of drag, cooling at low air speeds, and better cooling of the engine accessories. The drag of the N.A.C.A. cowling can be reduced materially if the bluntness of the nose is eliminated. Cooling at low air speeds can be improved if the propeller slipstream is utilized to a better advantage; the cooling air should be taken in at the point of highest pressure. The engine accessories can be kept cool if the air is passed over them before entering the engine cylinder baffle passages. These requirements define the wing-duct cooling system described.

The purpose of the present investigation is to determine the practicability of the wing-duct cooling system, but not necessarily to formulate a basis for all design requirements.

APPARATUS AND METHODS

The tests were conducted in the N.A.C.A. 20-foot propeller-research tunnel described in reference 2. In view of the preliminary nature of the tests, no new basic apparatus was constructed except the cowlings and entrance ducts. The wing used is a relic of previous wing-nacelle tests and not well suited owing to the high camber. A photograph of the set-up is shown in figure 1 and a drawing is given in figure 2.

Wing.- The wing, described in reference 3, is of wood construction having a span of 15 feet and a chord of 5 feet. The maximum thickness is 1 foot or 20 percent of the chord. The section is a Fokker design with a flat lower surface. The camber is therefore 10 percent, based on the lower surface chord line, or somewhat less if based on a chord line passing through the center of the leading-edge radius. The aerodynamic characteristics of this wing section differ considerably from sections now used, in that zero lift occurs at -8° angle of attack whereas it occurs at -1° or -2° for the low-cambered sections now in extensive use. The operating lift coefficient of this wing for cruising speeds should not be considered the same as for modern wings because of this marked difference in angle for zero lift. This wing should operate at a higher lift coefficient.

The operating lift coefficient has an important bearing on this analysis because the drag due to the entrance ducts is sensitive to angle change, particularly in the negative angle range. The ducts were located in a place to give the highest pressure (stagnation point) when the wing was at an angle of attack of 0°. The angle of 0° was selected because it approximated the operating angle for present-day wings, particularly for the portions of the wing within the slipstream.

Cowlings.- The cowlings were formed from sheet aluminum. An outline of the basic cowlings, differing only in the shapes of the nosepieces and locations of the exit slots, is shown in figures 2 and 3. Cowling 39 is intended to have a spinner nose attached to the propeller hub, but a spinner was not made because one was not considered essential for the present tests.

The exit slot width was varied from 0 to 1-1/2 inches by moving the nosepieces in a fore-and-aft direction. The slot width was measured across the minimum distance, rather than the fore-and-aft distance. In general, the basic cowling lines formed a nearly continuous curve across the exit slot except for cowlings 3B, 3D, and 3C, which were of the overlapping type. Cowling flaps, as a means of opening the exit slot, were not tested.

Entrance ducts.- The basic shapes of the wing-duct entrances are shown in figure 4. Three basic shapes were tested, all having an area at the mouth of 25 square inches for each entrance; a square one extending slightly

in front of the wing, an elliptical one of the extended type, and a square one flush with the wing surface. The square extended one was modified by rounding the top surface with plasticine. The extended elliptical one was modified by moving it back 1 inch. The modifications to the square flush entrance are shown in figure 5, consisting essentially of increasing the lip radii of the upper and lower surfaces.

Two wing ducts were used, one on either side of the nacelle located at about 0.71 of the propeller tip radius. Subsequent tests on a full-scale propeller set-up indicated that higher pressures in the entrance could have been realized for ground cooling had the openings been closer to the nacelle.

The size of the ducts was arbitrarily determined from considerations of the dimensions of the wing and nacelle. The question of size, from the standpoints of the drag and the internal losses, is a subject needing amplification.

The internal-duct passages are 5 inches square in cross section at the mouths and are rectangles, 6 inches high and 7 inches wide, at the exits into the nacelle. Each passage makes one 90° turn. Four equally spaced guide vanes were provided in each turn to conduct the air around the corner without excessive losses. Other than the expanding ducts and the guide vanes provided, no attempt was made to reduce the internal-duct losses. The air passed from the ducts into each side of the large space provided by the nacelle, and there was no attempt to convert the kinetic energy in the streams into pressure energy at those points.

The reason no great pains were taken in the design of internal-duct shape was because that phase of the subject is better handled on a simplified set-up using a blower to force air through the passages rather than the wind tunnel. This part of the program is being continued and the results will be available soon.

In the present paper the restrictions imposed by the entrance ducts and the engine resistance are considered as one value, the total internal restriction (except for the exit slots). To use the data, the engine-baffle restriction must be separated from the entrance-duct restriction, as will be brought out later.

Equivalent baffle restrictions.- Engines of different power output require different quantities of cooling air for a given air temperature rise. In order to cover a wide range of engine sizes, removable orifice plates were provided. The plates were located at the points in the cooling-air circuit where the air passed from the ducts into the nacelle. These orifice plates simulated the resistances of engines ranging from about 300 horsepower to about 1,500 horsepower. A few tests were made with an orifice plate located in the usual place for a radial engine.

The quantity of air flowing was determined from calibrations involving the pressure drops across the orifice plates. The orifice plates were calibrated by drawing air through the system and also through a calibrated venturi tube by means of a blower.

Motor and propeller.- The propeller was driven by a 25-horsepower electric motor turning at various speeds up to 3,600 r.p.m. The propeller used for most of the tests is a 4-foot model of the 3101 three-blade propeller. A few tests were made with a 4-foot model of the 4412 two-blade propeller. The three-blade propeller was set at 20° blade angle at the 0.75 radius for nearly all of the tests because this angle nearly represents that for the take-off and climbing conditions of many present-day airplanes. The effect of blade angle was determined for one cowling by operating the propeller at angles ranging from 15° to 35°.

SYMBOLS

Q, quantity of cooling air, cu. ft. per sec.

A_e, equivalent engine orifice area (orifice coefficient = 1.0), sq. ft.

A_d, Equivalent entrance duct orifice area, sq. ft.

A_c, projected area of the engine, sq. ft.

K_e, conductivity of engine, A_e/A_c, $\dfrac{Q}{A_c\sqrt{\dfrac{2\Delta p_e}{\rho}}}$

K_d, conductivity of entrance duct, A_d/A_c, $\dfrac{Q}{A_c\sqrt{\dfrac{2\Delta p_d}{\rho}}}$

K_t, total conductivity of entrance duct and engine,

$$\frac{Q}{A_c\sqrt{\dfrac{2\Delta p_t}{\rho}}} \qquad \frac{1}{K_t^2} = \frac{1}{K_e^2} + \frac{1}{K_d^2}$$

Δp_e, pressure drop across engine orifice, lb. per sq. ft.

Δp_d, pressure drop across entrance duct, lb. per sq. ft.

Δp_t, pressure drop across the entrance duct and the engine baffles.

ΔD_a, drag added due to slowing down the cooling air, lb.

$$\Delta D_a = \frac{\Delta p_t Q}{V}$$

ΔC_{D_a}, drag coefficient for cooling air drag,

$$\Delta C_{D_a} = \frac{\Delta p_t Q}{\frac{1}{2}\rho V^3 A_c} = \left(\frac{\Delta p_t}{q}\right)^{3/2} K_t$$

η_a, efficiency of the cooling system, $\left(\dfrac{\Delta p_e}{q}\right)^{3/2} \dfrac{K_e}{\Delta C_{D_t}}$

ΔD_i, interference drag due to air entering and leaving the cowling.

ΔD_t, total drag added due to the cooling air, $\Delta D_a + \Delta D_i$.

$$\Delta C_{D_t} = \frac{\Delta D_t}{qA_c}$$

D_p, total nacelle drag including total cooling-air drag (ΔD_t) and the drag of the square entrance ducts (faired).

C_{D_p}, total nacelle drag coefficient, $= \frac{D_p}{qA_c}$

ρ, mass density of the air, slugs per cu. ft.

V, velocity of the airplane.

K_p, pressure coefficient with propeller operating,

$$K_p = \frac{\Delta p_t}{\rho n^2 D^2}$$

n, rotational speed of the propeller, rev. per sec.

D, propeller diameter, ft.

$C_{D_{(W+N)}}$, drag coefficient of the wing with the nacelle.

$C_{L_{(W+N)}}$, lift coefficient of the wing with the nacelle.

p_e, pressure in the mouth of the entrance ducts, lb. per sq. ft.

RESULTS AND DISCUSSION

The success or failure of any radial-engine cowling lies chiefly in the drag that it adds to the minimum airplane drag and the effectiveness with which the engine is cooled under all operating conditions. The cooling problem is generally confined to the low-air-speed and high-altitude conditions of flight because there is usually little difficulty in cooling engines at cruising speeds.

Cooling an engine is essentially a problem of forcing air through the baffle passages. If the quantity of air necessary to cool an engine is known and also the pressure necessary to force that quantity through the baffles, the problem may be resolved into one of simple fluid mechanics. The engine-baffle passage may be considered as an orifice placed in a tube of diameter equal to the engine diameter. The quantity of air flowing through the equivalent engine orifice, which is assumed to have a coefficient of unity, is

$$Q = A_e \sqrt{\frac{2\Delta p_e}{\rho}}$$

A_e/A_c is then defined as the engine "conductivity," K_e. Theodorsen in reference 4 develops this formula in a somewhat different manner.

In the wing-duct system there are two other restrictions in the flow passage, the entrance ducts and the exit slot. Although each may be considered as an orifice, it was found that only the entrance duct could conveniently be treated as such. The exit can better be treated as a slot of certain actual dimensions, rather than a fictitious area. The effective conductivity of the engine baffles and the entrance ducts, which are in series in the flow passage, is given by the relation

$$\frac{1}{K_t^2} = \frac{1}{K_e^2} + \frac{1}{K_d^2}$$

The problem of testing and presenting the data for the various modifications of each cowling is greatly simplified by using K_t instead of K_e and K_d separately. The data are likewise more useful in this form. The tunnel tests were made with a wide range of K_t values.

The drag of a cowling may be divided into three parts: (a) basic form drag of the nacelle or body, (b) drag due to slowing down the mass of air which enters the cowling to cool the engine, and (c) drag due to the disturbance of the flow over the cowling and wing as a result of the cooling air entering and leaving the system. The basic form drag is measured by closing the exit slot, which reduces the cooling-air flow to zero. The drag added by slowing down the cooling air cannot be measured directly, but can be calculated from the expression

$$\Delta D_a = \frac{\Delta p_t Q}{V}$$

if it is assumed that the loss of energy in the flow through the exit slot is zero.

In coefficient form,

$$\Delta C_{D_a} = \frac{\Delta p_t Q}{\frac{1}{2}\rho V^3 A_c}$$

Since

$$K_t = \frac{Q}{A_c \sqrt{\frac{2\Delta p_t}{\rho}}}$$

then

$$\Delta C_{D_a} = \left(\frac{\Delta p_t}{q}\right)^{3/2} K_t$$

In computing the efficiency of the system, that is, the useful power for cooling divided by the power expended, only the energy lost through the engine baffles should be considered.

$$\eta_a = \frac{\Delta p_e Q}{\Delta D_t V} = \left(\frac{\Delta p_e}{q}\right)^{3/2} \frac{K_e}{\Delta C_{D_t}}$$

The efficiency is not stressed in this paper because the pressure drop across the engine is not separated from the total pressure drop across the engine and entrance ducts, and also because there is some question as to what should be the basis of computing the drag increment. There seems to be no justification for using the no-flow drag of each cowling as a basis because then the poorest cowlings from the drag standpoint may have the highest efficiency, an obviously misleading condition. Stress is placed rather on the toal drag for given pressures available, which accomplishes the same purpose as the efficiency method.

The pressure available across the engine baffles and entrance ducts with propeller running is given in coefficient form,

$$K_p = \frac{\Delta p_t}{\rho n^2 D^2}$$

This coefficient is the criterion of cooling effectiveness because the propeller produces most of the pressure available at the low air speeds.

In the study of the shape of the duct entrances the criterion of the best entrance from the drag viewpoint is the drag for a given lift of the wing. The criterion for the effectiveness of the entrance in scooping in air is the pressure available in the mouth of the entrance, P_e and $P_e/\rho n^2 D^2$. (The latter form is preferred for low values of V/nD, propeller operating.)

Cowling Nose Results

Figures 6 to 22 give the test results for the various cowling nose shapes tested. The results are given in two types of curves. The criterion of efficiency is given in the form of $\Delta p_t/q$ plotted against C_D for different values of conductivity, K_t, and different exit slot openings. (The exit-slot width was always measured as the minimum distance across the exit slot, in inches. It should be borne in mind that these distances should be scaled in proportion to the cowling diameter for full-scale work. Slot width for full-scale equals the $\frac{\text{diameter of the full-scale cowling in inches}}{20}$ times the slot widths given in this paper.) The criterion for pressure available is given in the form of K_p plotted against V/nD.

Drag comparison.- In figures 23 to 25, comparisons are made of the various cowlings from the drag standpoint for three flow quantities, or values of K_t. The most interesting portion of the curves from the drag standpoint is that for low values of $\Delta p_t/q$, 0.2 to 0.5, because these values correspond to the cruising or high-speed flight conditions. The highest values of $\Delta p_t/q$ obtainable correspond to the take-off and climb and are of some interest from the cooling standpoint, although the results with propeller operating are more applicable.

Cowling 39 has the lowest drag for the high-speed range of the curves with cowling 3 or 3B taking second place. Cowling 3B, which has an overlapping exit slot,

shows up well for high values of $\Delta p_t/q$, even in the high-speed range. Small amounts of overlap of the exit seem desirable for large conductivities.

Cowlings 3C and 3D have an excessive amount of overlap, as may be seen from figure 24. Cutting off parts of cowlings 3B and 3C, thereby locating the exit slot on the curved portions of the noses, had a detrimental effect.

The effect of the blunt nose of cowling 1 is apparent since it has a high drag in the high-speed range. The maximum pressure available is less than for other forms, indicating the rear location of the exit slot is not conducive to high pressures. Cowling 5 is poor from both the drag and pressure standpoints.

The one test of an N.A.C.A. cowling with the exit slot closed indicates that it is inferior to the other cowlings tested, even though the wing-duct results include the drag of the square extended entrances (faired). The accuracy of the tests, however, was not such as to make extremely fine comparisons because the cowlings constituted only about 5 percent of the total drag of the set-up. One-half percent error in the total drag would mean 10-percent error in the cowling drag.

Following is a table giving the efficiencies, together with the values used in the computations, for cowling 39. The computations cover three values of K_t, all taken at a value of $\Delta p_t/q$ of 0.8. The duct conductivity, K_d, is the one existing during the tunnel tests, although this value need not apply to an airplane installation.

K_t	0.0469	0.0778	0.1178
K_d	.1775	.1775	.1775
K_e	.0487	.0867	.157
$\Delta p_t/q$	.8	.8	.8
$\Delta p_e/q$	.744	.647	.448
ΔC_{D_t}	.040	.070	.108
η_a	.78	.65	.44

It may be noted that the efficiency decreases as the quantity of air is increased, due primarily to the increased losses in the entrance ducts. For example, nearly half of the pressure available is lost in the entrance duct for the highest engine conductivity, K_e, while only a few percent are lost for the lowest.

If perfect entrance ducts were possible, a condition which can be approached for large sizes or ideal expanding conditions, the above table could be modified as follows:

K_t	0.0469	0.0778	0.1178
K_d	∞	∞	∞
K_e	.0469	.0778	.1178
$\Delta p_t/q$	.8	.8	.8
$\Delta p_e/q$	.8	.8	.8
ΔC_{D_t}	.040	.070	.108
η_a	.84	.79	.78

These tables draw attention to the importance of efficient entrance ducts for high flow conditions. This subject will be discussed more fully later.

Cooling comparisons.- A comparison of the cowlings from the cooling standpoint is given in figures 26 to 28 for the condition of zero air speed.

The results indicate that for ground cooling, wide overlapping exit slots located on or near the maximum leading-edge curvature produce the greatest pressure. The exit slot for cowling 5 is evidently too close to the propeller axis (positive-pressure region) to produce a reasonably high pressure drop.

Cowling 39 was not tested with the propeller operating owing to the fact that the nose part would have had to be a spinner and this would have entailed a certain delay for the manufacture. It is believed that the cooling characteristics can be approximated fairly closely, however, from the other tests of cowlings having similar exit slot openings. For example, the cooling characteristics for cowling 39 should approximate those for cowlings 1 and 3, or cowling 3B if a small overlap were provided.

The pressure available in the take-off and climb is always greater than that for the ground condition, depending, of course, on the air speed or V/nD. No comparisons are made for these conditions because the ground-cooling criteria are probably indicative of the relative merits of the cowlings for the take-off and climb also.

Effect of propeller-blade setting and angle of attack of the wing.- Most of the propeller tests were made at a blade angle of 20° at 0.75 radius, because this represents the blade angle for the take-off condition of most present-day airplanes. In figure 29, the results from tests at other blade settings are given for one cowling. Increasing the blade angle increases the pressure available in a nearly uniform manner except for the zero V/nD condition.

Increasing the angle of attack of the wing from 0° to 10° increases the pressure slightly at low values of V/nD and more so at high values.

Entrance Ducts

The design of efficient entrance ducts is probably

the most difficult part of the wing-duct cowling system. The three important elements to consider are: (a) the drag, (b) the pressure available in the entrance, and (c) the loss in head through duct. The location, size, and shape of the mouth affect the first two, while the size and shape of the interior duct affect the third.

The study of entrance ducts herein reported is by no means complete. Only one size and location of the entrance were investigated, although several basic shapes of the mouths were tested. The wing on which these tests were made is poorly suited for making a comprehensive study of entrance shapes owing to the extremely high camber. The present results, which are of a preliminary nature only, should be considered as qualitative until a more complete study can be made using a modern wing section.

Location.- The wing-duct entrances should be located along the span in such a position as to receive the greatest benefit from the propeller slipstream, especially in the take-off and climbing conditions. The pressure distribution in the slipstream of a propeller depends upon many factors, such as: blade angle, V/nD, distance behind the propeller disk, the pitch distribution, and the plan form. No study of the problem is made here except to point out that the slipstream necks down considerably behind the propeller for high disk loadings, such as are present during the take-off. Figure 30 shows the radial pressure distribution at 0.5 the diameter behind the propeller for the static condition. The maximum pressure occurred at 0.55 of the propeller radius for this condition, and decreased rapidly beyond the 0.6 radius. The peaks of these curves will broaden rapidly with increased air speed.

The vertical location of the entrances was determined for these tests from pressure-distribution measurements made with propeller operating. The region of maximum pressure dictated the location of the entrances although the one selected might not be the best from the drag standpoint.

Drag of entrances.- Polar curves for the entire setup are given in figures 31 to 34 comparing the various entrance shapes. The entrances were located on the wing for high-speed operation at an angle of attack of about 0°, irrespective of what the lift coefficient might be

for this particular high-cambered wing. In this way, the disturbances created by the entrances would approximate those for a lower-cambered wing actually operating at about 0°. The comparisons should be confined, therefore, to the angle-of-attack range above 0°.

Referring to figures 31 and 32, it may be seen that all the entrances have a slight drag at 0° angle of attack, but there is no measurable drag at about 3°. The extended entrances both improve the $C_{L_{max}}$. There seems to be little choice in the different entrance shapes in the angle range from 0° to 5°.

Figure 33 indicates that fairing the tops of the square extended ducts reduced the drag in the climbing range, but the effect was negligible at about 1°.

Modifying the flush square ducts by increasing the radii at the top and bottom of the entrances reduced the drag to a negligible amount, particularly in the negative-angle range. (See fig. 34.) The thin lower lip of the entrance accounts for the separation at the negative angles. The duct cross-sectional area was decreased by this process, however.

From these tests it appears that if the wing is thick in proportion to the entrance openings, flush ducts with well-rounded entrance lips will have no appreciable drag. If the wing is thin in proportion to the size of the entrance openings, extended scoops will probably be preferable because it is possible to incorporate well-rounded leading edges in the extended types, whereas this is not possible in the flush types without reducing the duct area. It is imperative that separation at the upper and lower lips be avoided even though the cross-sectional area of the ducts be decreased by so doing. Further work on this subject of entrance ducts is contemplated.

Pressure available in the entrance mouth.- It is obviously important that the entrance ducts be so shaped and located in such places that the maximum pressure can be obtained, particularly with the propeller running. From figures 35 and 36, it appears that the extended entrances provide the highest pressures within the angle range between -5° and 10° without the propeller operating. The flush entrances are equal only in the range of a few degrees near 0° angle of attack.

It may be surprising that pressures exceeding q are recorded. This can be accounted for by the fact that the static pressure in the tunnel jet at the model entrance ducts is higher than the average static pressure in the test chamber. The total head in the mouth of the entrance ducts referred to the average static pressure is therefore slightly in error by the amount noted (2 or 3 percent).

Referring to figure 37, it can be seen that modifying the flush entrances made the pressure more sensitive to angle-of-attack changes.

In figure 38 the basic ducts are compared with propeller operating. In the low V/nD range, corresponding to the take-off and climb, the square extended ducts are generally superior and the flush ducts are equally good over parts of the range. In general, there probably is not enough difference in all the ducts to warrant selecting one over the other on the basis of pressures available alone. The drag is of much more importance.

Internal properties of ducts.- The passages extending from the mouths of the entrance ducts to the engine compartment should convey the air with as little loss in energy as possible. There are two sources of energy loss: (a) friction or turbulence within the wing ducts, and (b) loss of kinetic energy in the stream at the point of "dumping" the air into the engine accessory compartment. It can be seen from Bernoulli's equation, $H_{total} = H_{static} + \frac{1}{2} \rho V_{duct}^2$, that both losses can be minimized if the velocity in the ducts is kept to a small figure or if the air is expanded efficiently upon entering the accessory compartment. Some interesting results taken from reference 5 on the efficiency of diffusers are given in figure 39. The entrance-duct conductivity, K_d, is a measure of the over-all efficiency of the ducts. If the losses are zero, the conductivity is infinite.

Figure 40 shows the loss in total head across the entrance ducts for the test conditions and for improved ducts.

Curves showing the relationship between K_t and K_e are given in figure 41 for two values of K_d. The tunnel test results can readily be translated into values of K_e and Δp_e for the two entrance-duct conductivities, $K_d = 0.1775$ and $K_d = 0.25$.

If the duct-pressure losses are to be kept to a certain fraction of the total pressure available, the entrance conductivity must bear a certain relation to the total conductivity or engine conductivity. Following is a table of relative conductivities for various pressure ratios.

$\Delta p_e/\Delta p_t$	K_d/K_t	K_d/K_e
1.0	∞	∞
.9	3.16	2.98
.8	2.24	2.00
.7	1.83	1.53
.6	1.58	1.22
.5	1.41	1.00

In equation form,

$$\frac{K_d}{K_t} = \frac{1}{\sqrt{1 - \frac{\Delta p_e}{\Delta p_t}}}$$

and

$$\frac{K_d}{K_e} = \frac{K_d}{K_t}\sqrt{\frac{\Delta p_e}{\Delta p_t}}$$

From the above values or equations the sizes of the entrance ducts can easily be computed knowing: K_e, Δp_e, Δp_t, and K_d. The value of K_d must be gotten from tests of ducts of given sizes. For example, if the pressure across the engine, Δp_e, must be at least 0.8 the total pressure available, Δp_t, the entrance-duct conductivity must be at least 2.0 times the engine conductivity. If the relationship between the entrance size and its conductivity is known (from test results), the actual size can be determined directly.

The wing ducts for the test set-up were square in cross section and made one 90° turn. The area of each duct increased somewhat during the turn. No attempt was made to extend the duct into the nacelle proper. Guide vanes in the 90° turn increased the conductivity from about 0.12 to 0.1775. Other than this single test with guide vanes, no attempt was made to increase the conductivity of the wing ducts while the set-up was in the tunnel. Research is being continued, however, with a simplified set-up using a blower to draw air through various types of ducts. The results of this work will be given when completed.

Use of Data

It should be recognized that the present tests are of a preliminary nature and are lacking, therefore, in completeness and refinement. The results are not without considerable value, however, and should prove to be of aid in developing or designing cowlings of this type. The following procedure is suggested.

Selecting entrance ducts.- The conductivity of the entrance ducts must be first established. The shape and size will depend upon the airplane in question. The larger the ducts the less will be the internal losses and the greater will be the pressure available across the engine. Unless the wing is very thick, large entrances may prove too expensive from the drag standpoint. The present ducts are 5 inches in height and the maximum wing thickness is 12 inches. The height probably should not exceed 0.5 the wing thickness, but the width could be greater. The entrance duct conductivity should be at least twice that of the engine. If little expansion in the ducts is possible, from the entrance to the engine compartment, the area of each entrance should then be about equal to the equivalent engine orifice area. The duct losses constitute then only 20 percent of the internal energy or pressure.

The success or failure of this type of cowling depends upon the wing ducts. Unless the wing is sufficiently thick to accommodate the required ducts, or unless it is possible to expand the air efficiently, this type of cowling may not prove to be enough better than other types to warrant the extra cost and complications.

Selecting a cowling nose shape.- The shape of the nose will depend primarily upon whether or not a spinner is to be used. The width and shape of the exit slot will depend upon the cooling requirements for the various flight conditions. It is obviously necessary to control the slot width to obtain the best performance at all speeds. A fore-and-aft method of opening the slot was used in the tests because good results were obtained and the drag was undoubtedly less than it would have been had flaps been used.

With the engine and entrance conductivities known, the drag results may be referred to in order to select the best cowling for the conditions, and the pressures for cooling can be obtained from the pressure-coefficient curves with propeller running.

Chart for converting K_p into pressure.- It can be seen from the equation

$$\text{pressure} = K_p \rho n^2 D^2$$

that the pressure is proportional to a constant times the propeller tip speed squared for standard atmosphere. As the tip speed is usually known, the pressure can be read from a chart directly in terms of water head. (See fig. 42.) This type of chart is convenient for making rapid calculations in preliminary work.

Example design.- Given

Δp_e = 6 inches H_2O

K_e = 0.10

Propeller tip speed for climb = 900 ft./sec.

Propeller tip speed for take-off = 950 ft./sec.

High speed V/nD = 1.5

Wing thickness sufficient to provide entrance ducts having K_d = 0.25

Then K_t = 0.0927 and $\frac{\Delta p_e}{\Delta p_t}$ = 0.862.

To design a suitable cowling:

Cowling 39 is selected. As a propeller was not tested with this nose shape, the K_p must be estimated from tests of cowlings 1 and 3.

Ground cooling.- From figures 8 and 12, $K_p = 0.178$ for 1.5-inch exit opening.

From figure 42,

$$\Delta p_t = 7.5 \text{ inches } H_2O$$

$$\Delta p_e = 7.5 \times 0.862 = 6.45 \text{ inches } H_2O$$

Take-off.- Assume take-off speed = 0.4 high speed.

$$\left(\frac{V}{nD}\right)_{\text{take-off}} = 1.5 \times 0.4 \times \frac{900}{950} = 0.568$$

$$K_p = 0.28$$

$$\Delta p_e = \frac{0.28}{0.178} \times 6.45 = 10.15 \text{ inches } H_2O$$

Climb.- Assume climbing speed = 0.6 high speed

$$\frac{V}{nD_{(\text{climb})}} = 0.9$$

$$K_p = 0.44$$

$$\Delta p_e = \frac{0.44}{0.178} \times 6.45 \times \left(\frac{900}{950}\right)^2 = 14.2 \text{ inches } H_2O$$

High speed.- The exit slot width would be reduced to obtain 6 inches H_2O.

In this example the ground cooling is considered satisfactory and that for take-off and climb more than satisfactory. If the ground cooling is not considered important, the entrance ducts could possibly be reduced in size if desired. The internal losses would increase, however.

CONCLUSIONS

The results of these preliminary model tests show that:

1. The wing-duct cowlings tested had appreciably less drag than a conventional N.A.C.A. cowling.

2. The pressures available for engine cooling at low air speeds ranged from 4 to more than 10 inches of water, depending chiefly upon the propeller tip speed, V/nD, cowling shape, and the flow restrictions imposed by the engine baffle and wing-duct passages.

3. The success of this type of cowling from either the cooling or drag standpoint depends upon whether the wing of the airplane in question is sufficiently thick to accommodate efficient ducts.

Langley Memorial Aeronautical Laboratory,
National Advisory Committee for Aeronautics,
Langley Field, Va., January 7, 1939.

REFERENCES

1. MacClain, A. Lewis, and Buck, Richard S.: Flight-Testing with an Engine Torque Indicator. S.A.E. Jour., vol. 42, no. 2, Feb. 1938, pp. 49-62.

2. Weick, Fred E., and Wood, Donald H.: The Twenty-Foot Propeller Research Tunnel of the National Advisory Committee for Aeronautics. T.R. No. 300, N.A.C.A, 1928.

3. Wood, Donald H.: Tests of Nacelle-Propeller Combinations in Various Positions with Reference to Wings. Part I. Thick Wing - N.A.C.A. Cowled Nacelle - Tractor Propeller. T.R. No. 415, N.A.C.A., 1932.

4. Theodorsen, Theodore, Brevoort, M. J., and Stickle, George W.: Full-Scale Tests of N.A.C.A. Cowlings. T.R. No. 592, N.A.C.A., 1937.

5. Patterson, G. N.: Modern Diffuser Design. The Efficient Transformation of Kinetic Energy to Pressure. Aircraft Engineering, vol. X, no. 115, Sept. 1938, pp. 267-273.

Figure 1.- Wing-duct cooling set-up.

Figure 2.- Outlines of wing-nacelle set-up with cowling 39.

Figure 3.- Basic cowling shapes.

Figure 4.- Basic entrance shapes.

Figure 5.- Modifications to the square flush entrance.

Figure 6.- Pressure available against drag for cowling 1. Square extended entrance, no propeller.

Figure 7.- Pressures available for cowling 1. 3/4-inch exit slot, propeller set 20°.

Figure 8.- Pressures available for cowling 1. $1\frac{1}{2}$-inch exit slot, propeller set 20°.

Figure 9.- Pressures available for cowling 1. $K_t = 0.0778$, propeller set 20°.

Figure 10.- Pressure available against drag for cowling 3. Square extended entrance, no propeller.

Figure 11.- Pressures available for cowling 3. 3/4-inch exit slot, propeller set 20°.

Figure 12.- Pressures available for cowling 3. $1\frac{1}{2}$-inch exit slot, propeller set 20°.

Figure 13.- Pressure available against drag for cowling 3B and 3B with $1\frac{1}{2}$ inches cut off. Square extended entrance, no propeller.

Figure 14.- Pressures available for cowling 3B. 3/8-inch exit slot, propeller set 20°.

Figure 15.- Pressures available for cowling 3B. 3/4-inch exit slot, propeller set 20°.

Figure 16.- Pressures available for cowling 3B. 1-1/4-inch exit slot, propeller set 20°.

Figure 17.- Pressures available for cowling 3B with $1\frac{1}{2}$ inches cut off. $K_t = 0.0778$, propeller set 20°.

Figure 18.- Pressure available against drag for cowling 3C and 3C with 1-1/4 inches cut-off. Square cut-off. Square extended entrance, no propeller, $K_t = 0.0778$.

Figure 19.- Pressures available for cowling 3C. $K_t = 0.0778$, propeller set 20°.

Figure 20.- Pressure available against drag for cowling 5. Square extended entrance, no propeller, $K_t = 0.0778$.

Figure 21.- Pressures available for cowling 5. $K_t = 0.0778$, propeller set 20°.

Figure 22.- Pressure available against drag for cowling 39. Square extended entrance, no propeller.
*Increased drag due to cooling air,

$$\Delta C_{D_a} = \left(\frac{\Delta p_t}{q}\right)^{3/2} K_t$$

Figure 23.- Pressure available against drag for different cowlings. Square extended entrance, no propeller, $K_t = 0.0469$.

Figure 24.- Pressure available against drag for different cowlings. Square extended entrance, no propeller, $K_t = 0.0778$.

Figure 25.- Pressure available against drag for different cowlings. Square extended entrance, no propeller, $K_t = 0.1178$.

Figure 26.- Pressure available at zero $\frac{V}{nD}$ for different cowlings. Propeller set 20°, $K_t = 0.0469$.

Figure 27.- Pressure available at zero $\frac{V}{nD}$ for different cowlings. Propeller set 20°, $K_t = 0.0778$.

Figure 28.- Pressure available at zero $\frac{V}{nD}$ for different cowlings. Propeller set 20°, $K_t = 0.1178$.

Figure 29.- Effect of various propeller blade-angle settings on K_p. Cowling 3, 3/4-inch exit slot, $K_t = 0.0778$.

Figure 30.- Radial pressure distribution in the slipstream at 0.5 propeller diameter behind the propeller disk. Three-blade propeller 5868-9 operating at zero $\frac{V}{nD}$. From full-scale tests with a liquid-cooled engine nacelle.

Figure 31.- Comparison of various entrance shapes. No air flow, cowling 3, 1-inch exit slot.

Figure 32.- Comparison of various entrance shapes. $K_t = 0.0778$, cowling3, 1-inch exit slot.

Figure 33.- Effect of fairing the top of the extended square duct. No air flow, cowling 3, 1-inch exit slot.

Figure 34.- Effect of modifying the square flush entrance. No air flow, cowling 3, 1-inch exit slot.

Figure 35.- Pressure available within differently shaped entrance ducts. No propeller, no air flow, cowling 3, 1-inch exit slot.

Figure 36.- Pressure available within differently shaped entrance ducts. No propeller, $K_t = 0.0778$, cowling 3, 1-inch exit slot.

Figure 37.- Pressure available within various flush entrance ducts. No propeller, no air flow, cowling 3, 1-inch exit slot.

Figure 38.- Pressure available within differently shaped entrance ducts. Propeller operating, 2-blade 4412 propeller set 13°, $K_t = 0.0778$.

Figure 39.- Efficiency of diffusers (from reference 5).

A, area. $\eta = \dfrac{p_2 - p_1}{\frac{1}{2}\rho V_1^2 \left[1 - \left(\frac{A_1}{A_2}\right)^2\right]}$

Figure 40.- Pressure across the engine in terms of total pressure available for different total conductivities.

Figure 41.- Engine conductivities for different total and entrance conductivities.

Figure 42.- Chart for converting pressure coefficient into pressure for different propeller tip speeds.

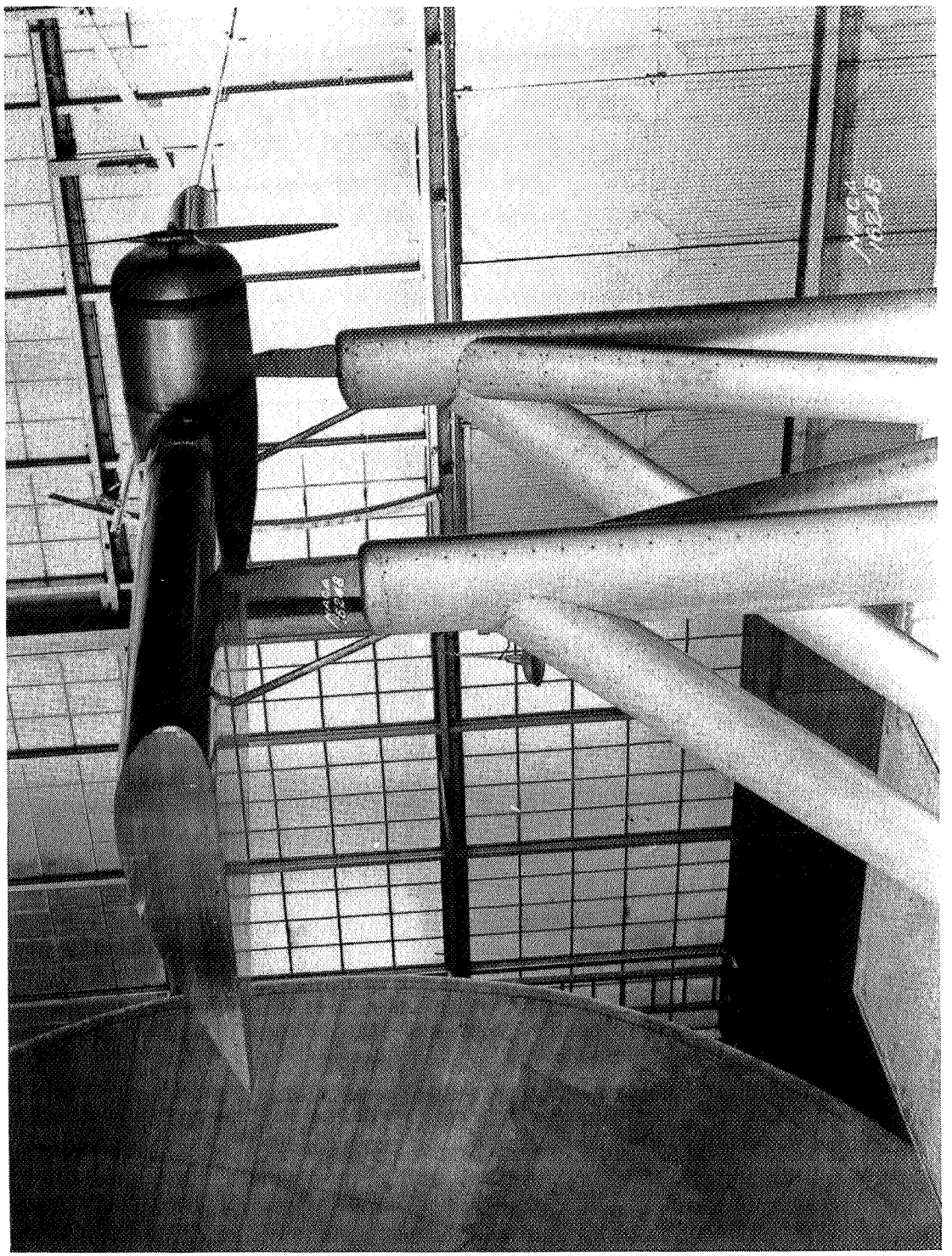

Figure 1.

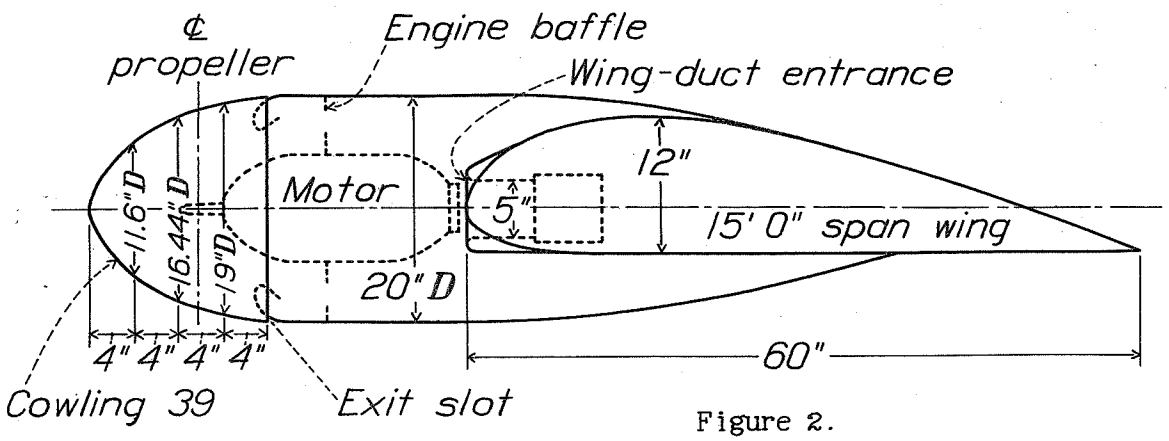

Figure 2.

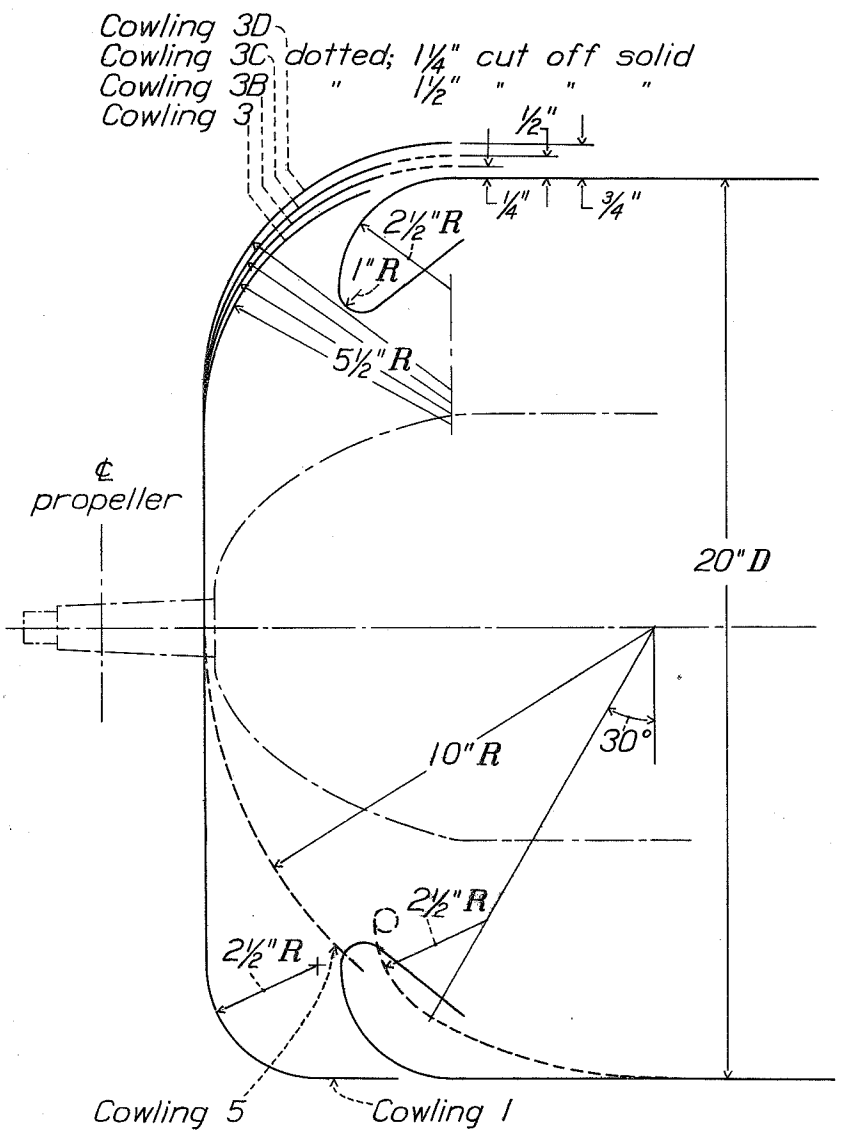

Figure 3.

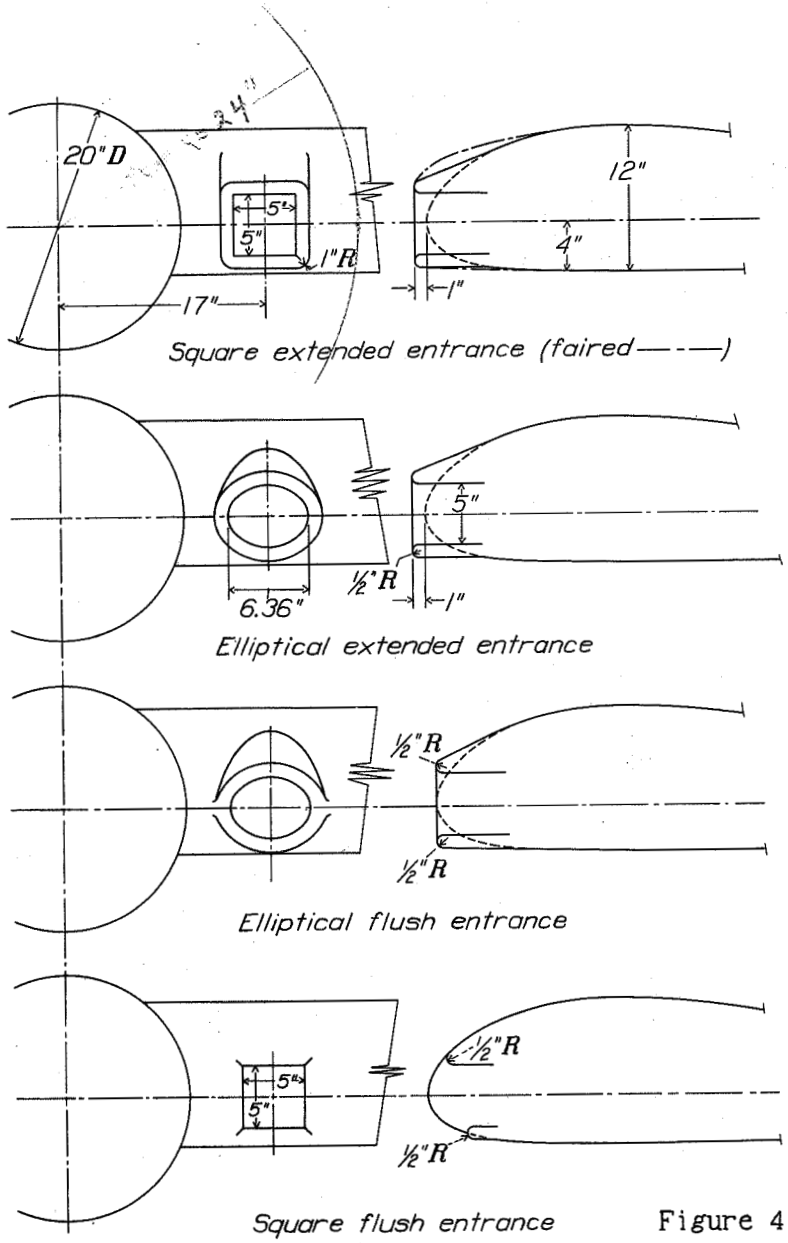

Figure 4

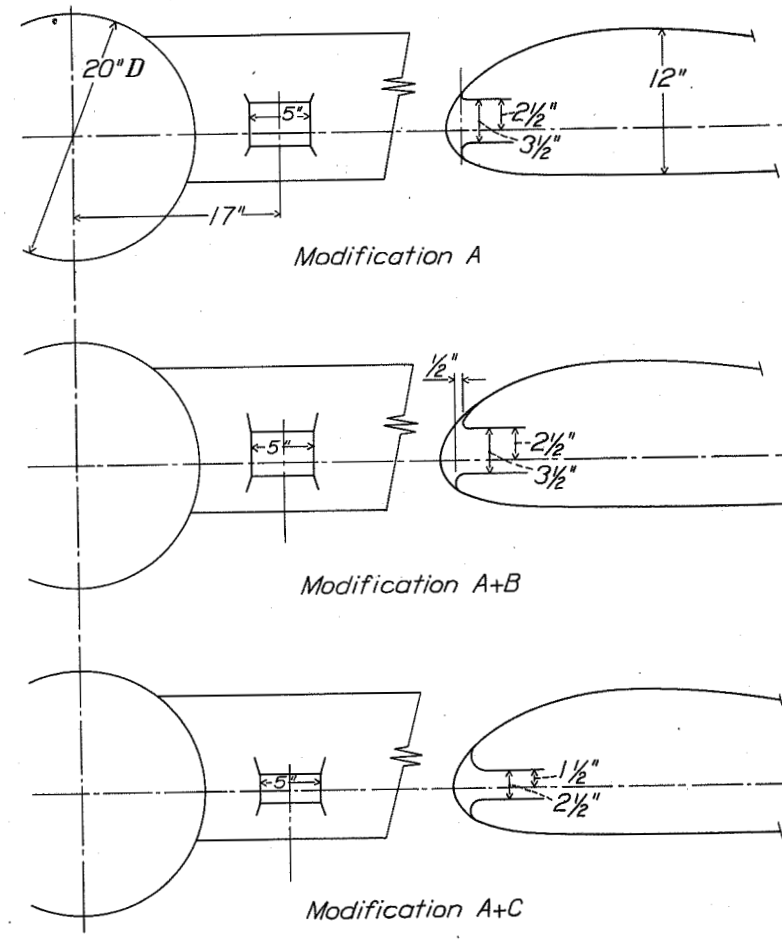

Figure 5

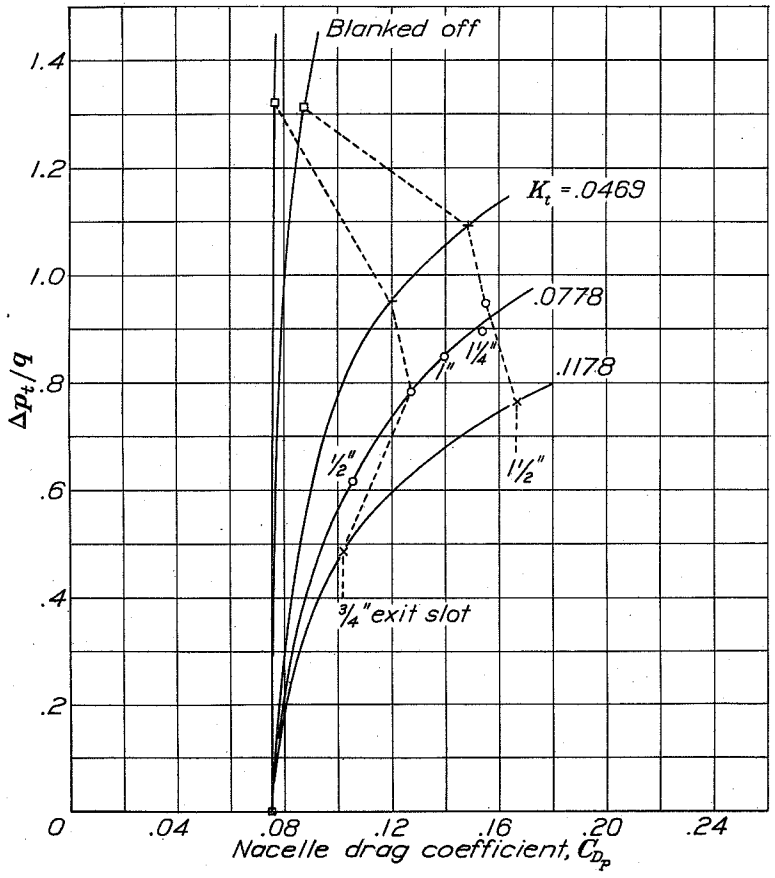

Figure 6.

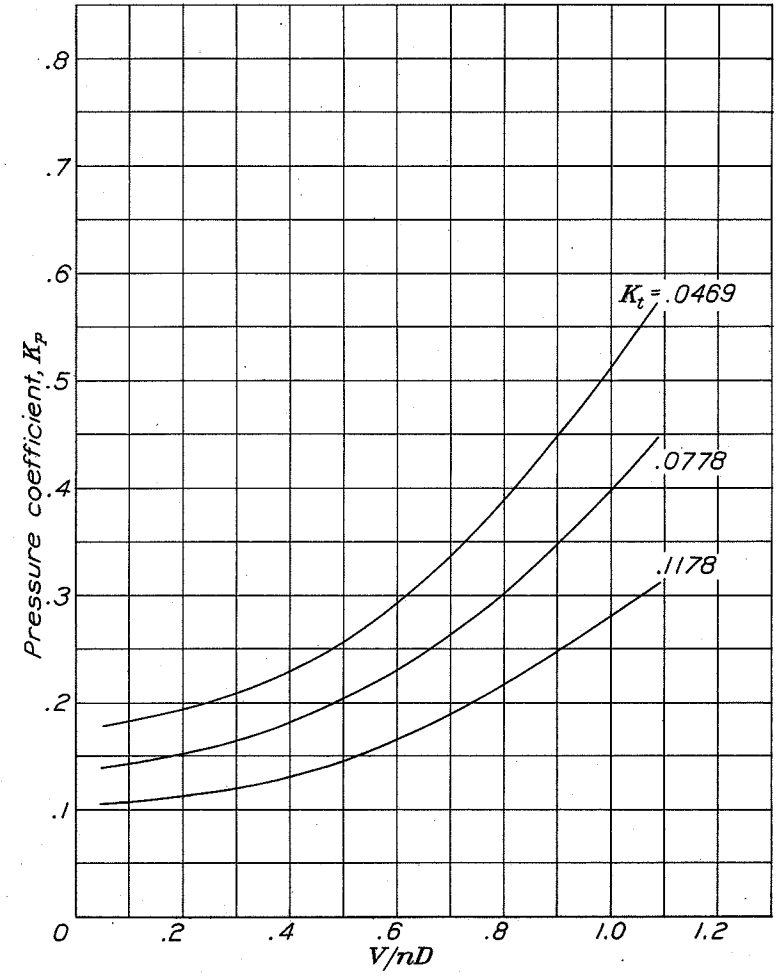

Figure 7.

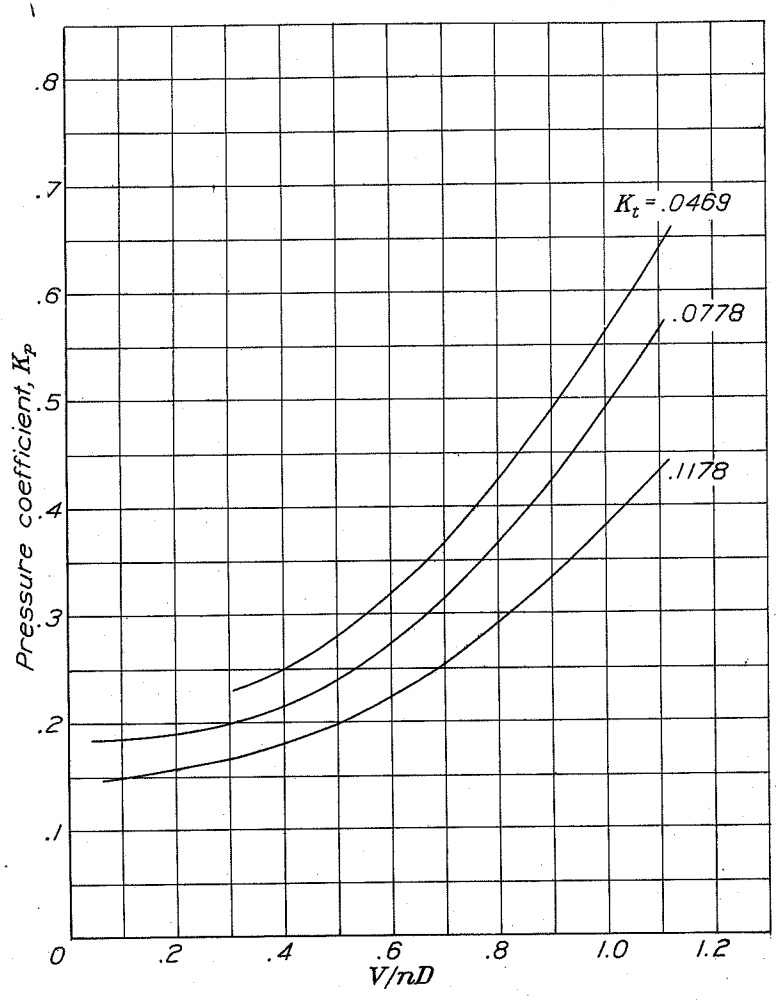

Figure 8.

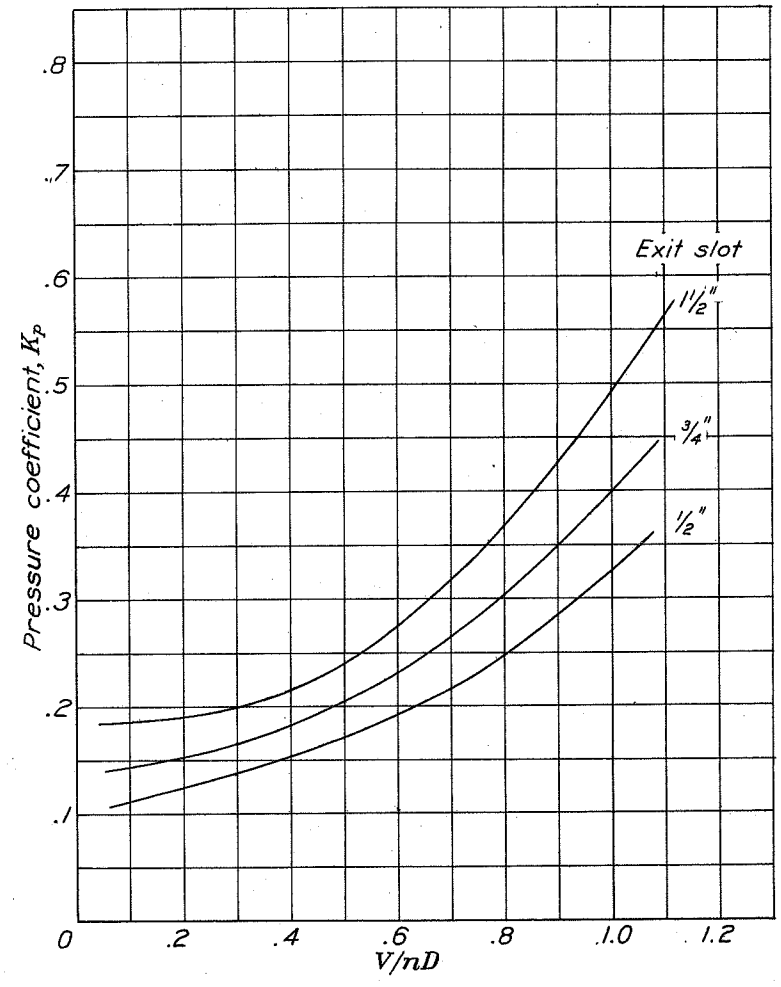

Figure 9.

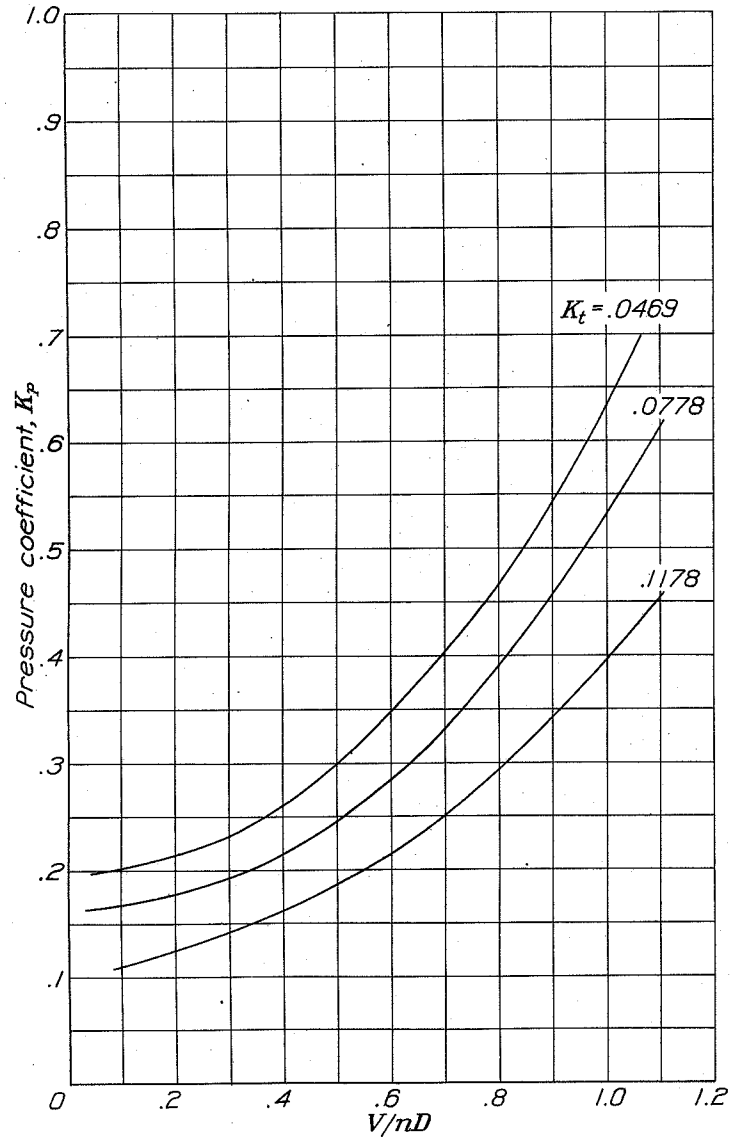

Figure 11.

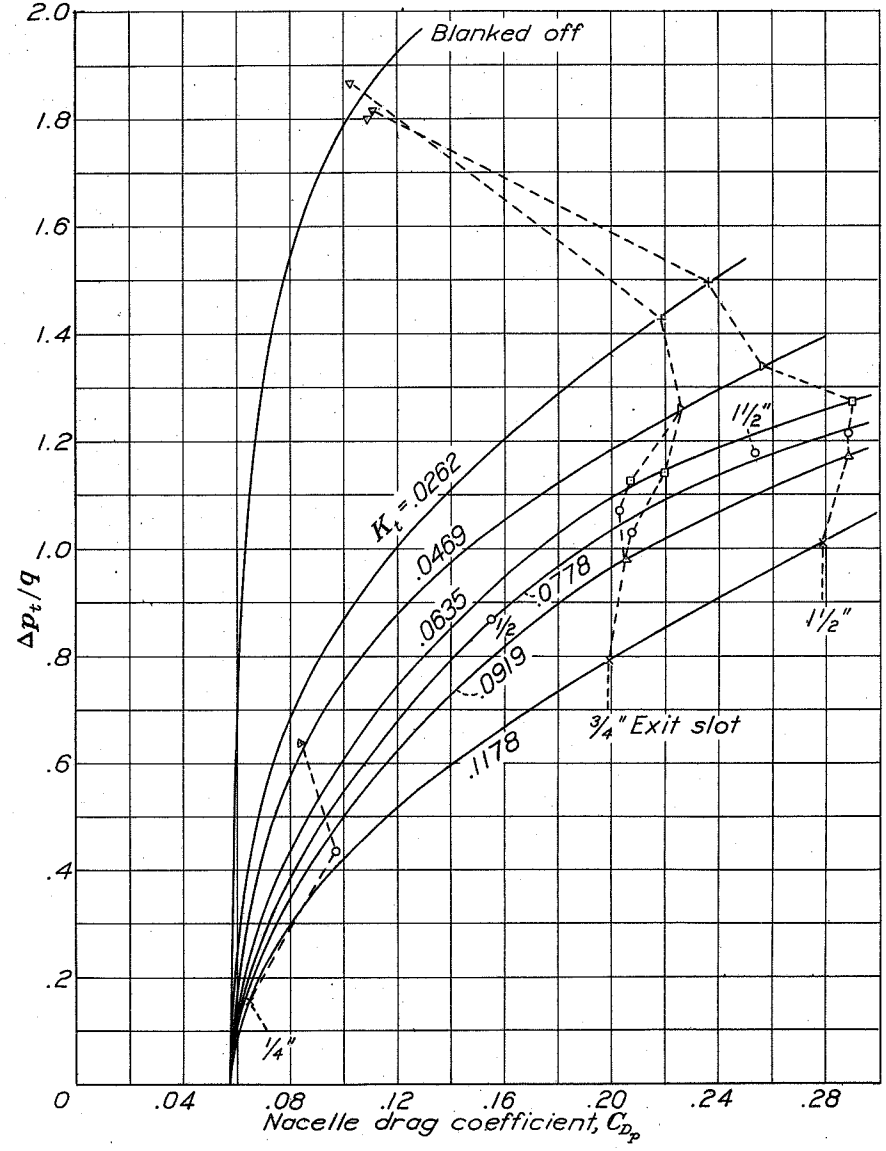

Figure 10.

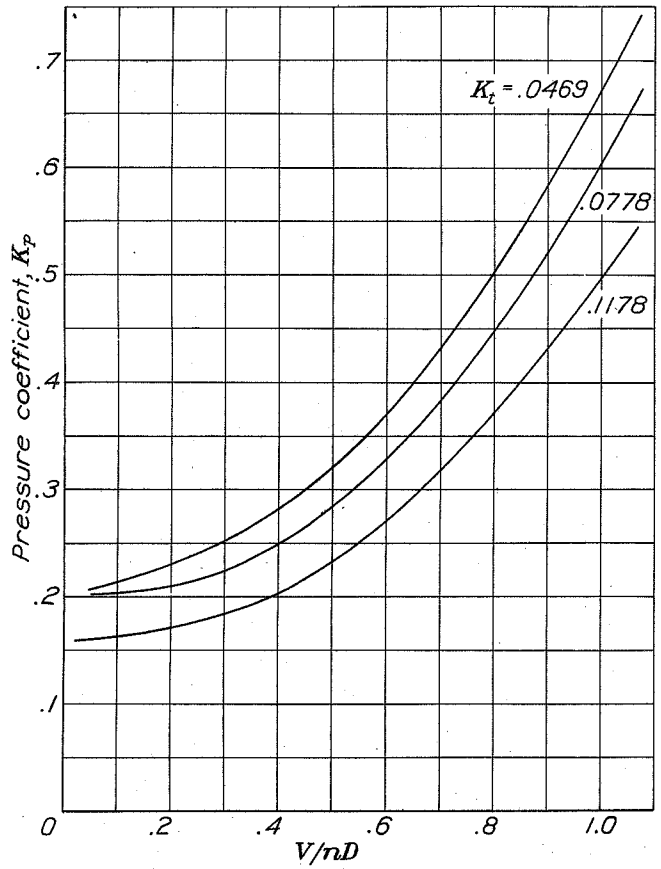

Figure 12.

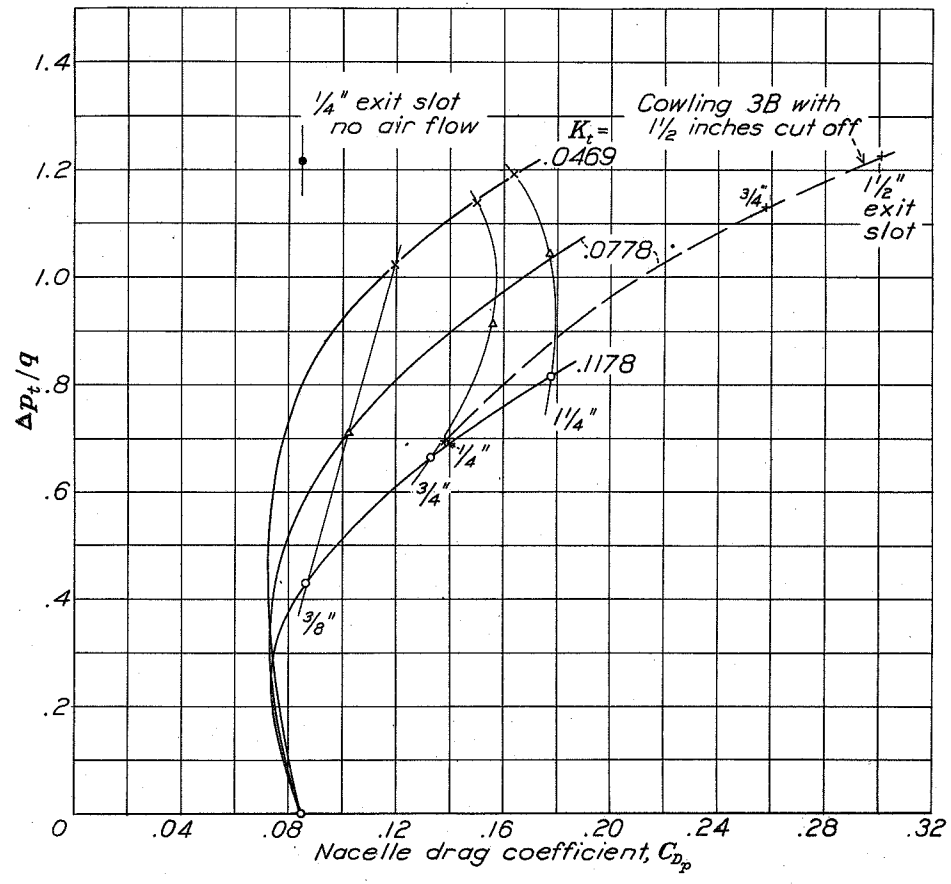

Figure 13.

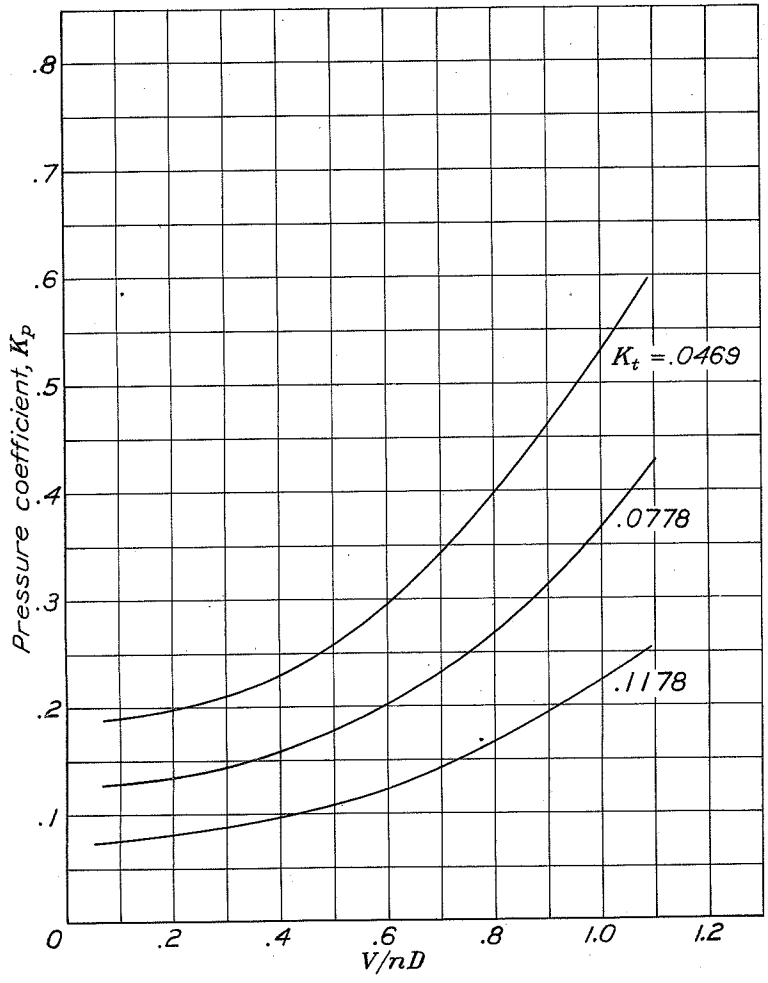

Figure 14.

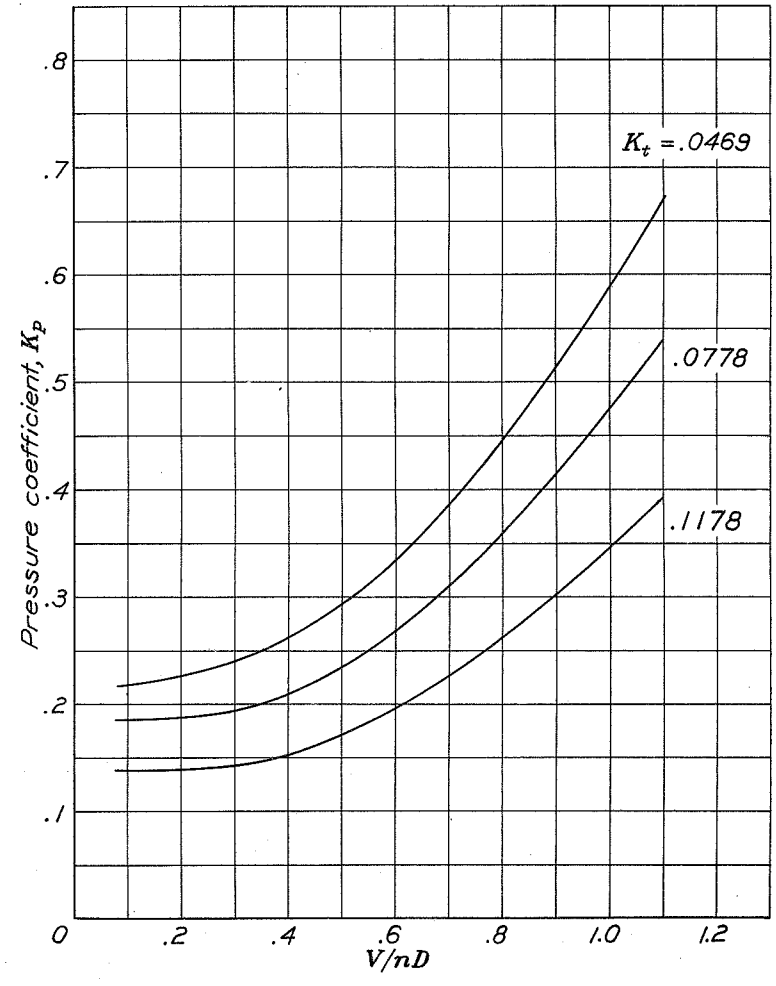

Figure 15.

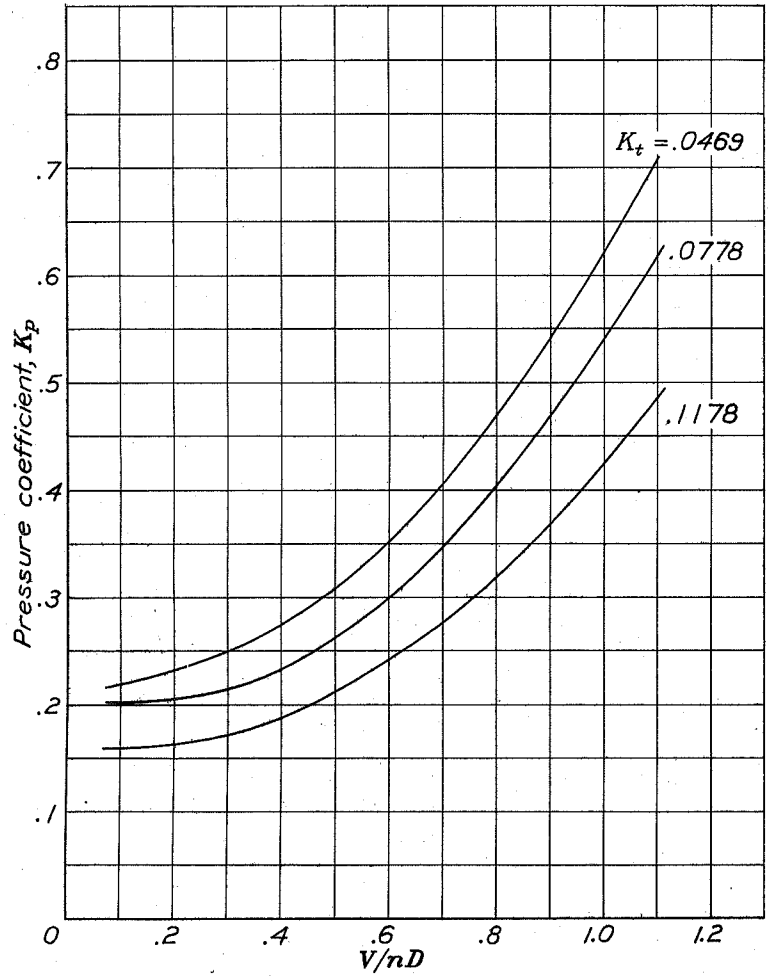

Figure 16.

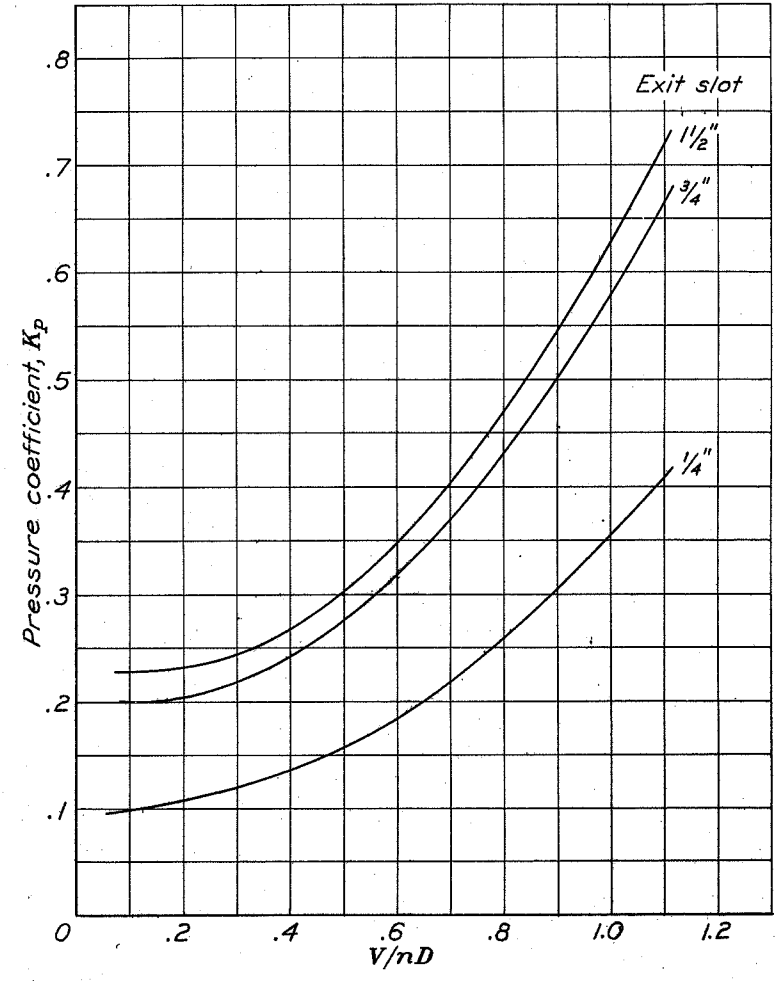

Figure 17.

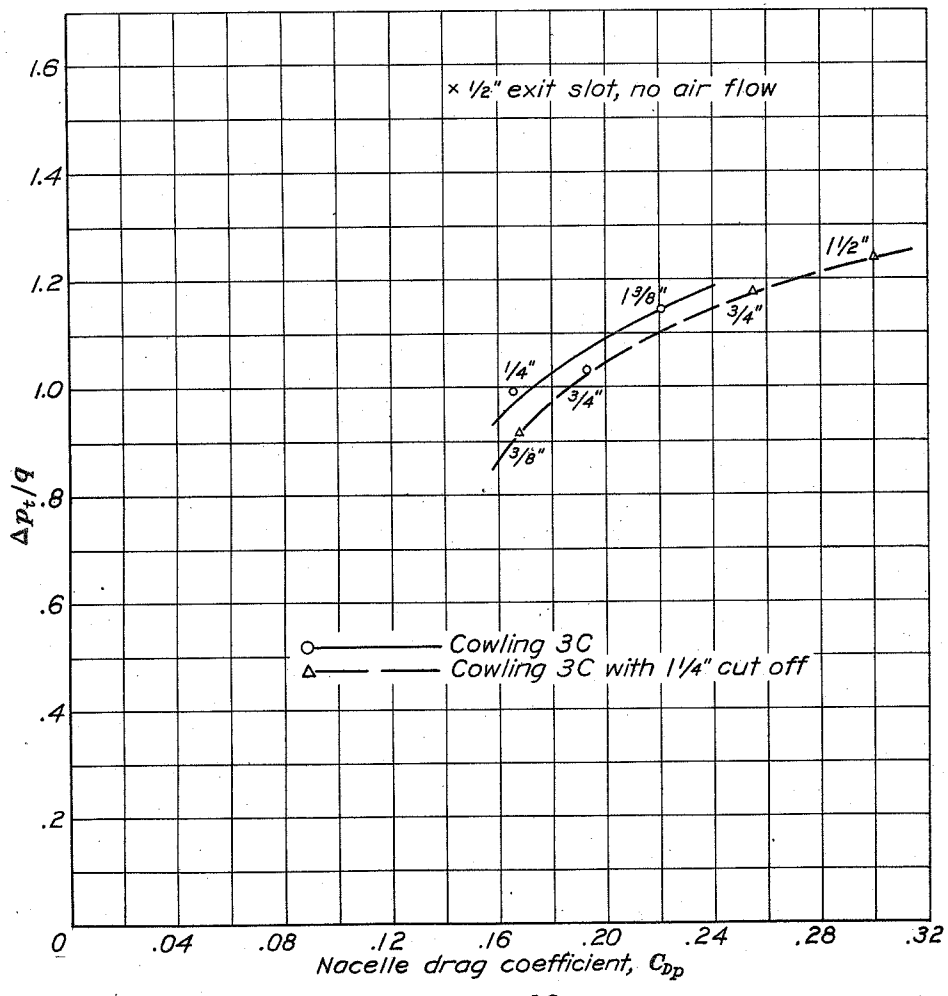

Figure 18.

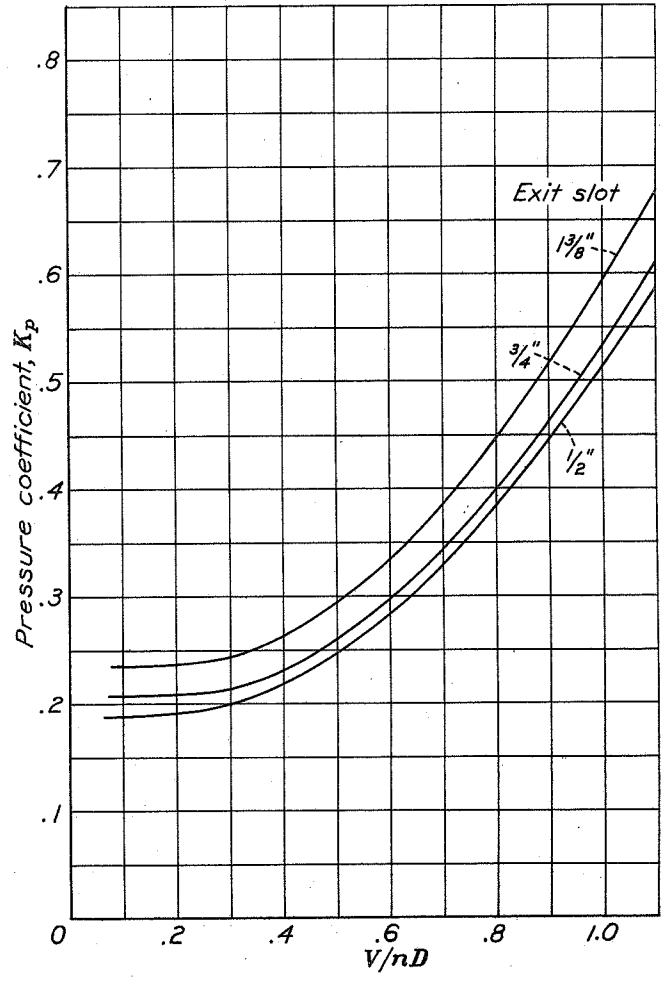

Figure 19.

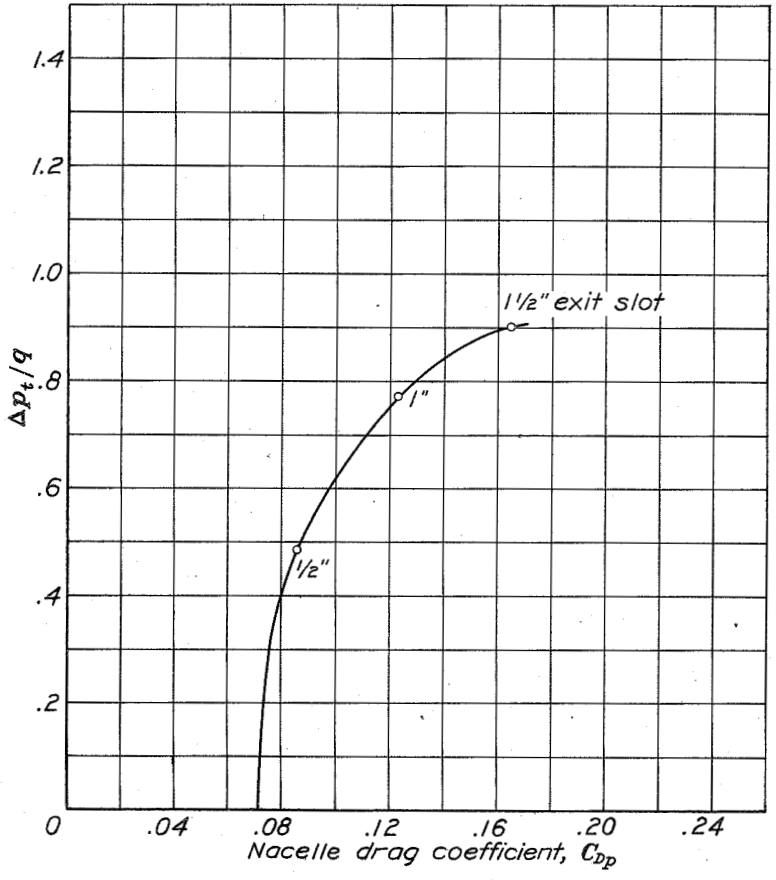

Figure 20.

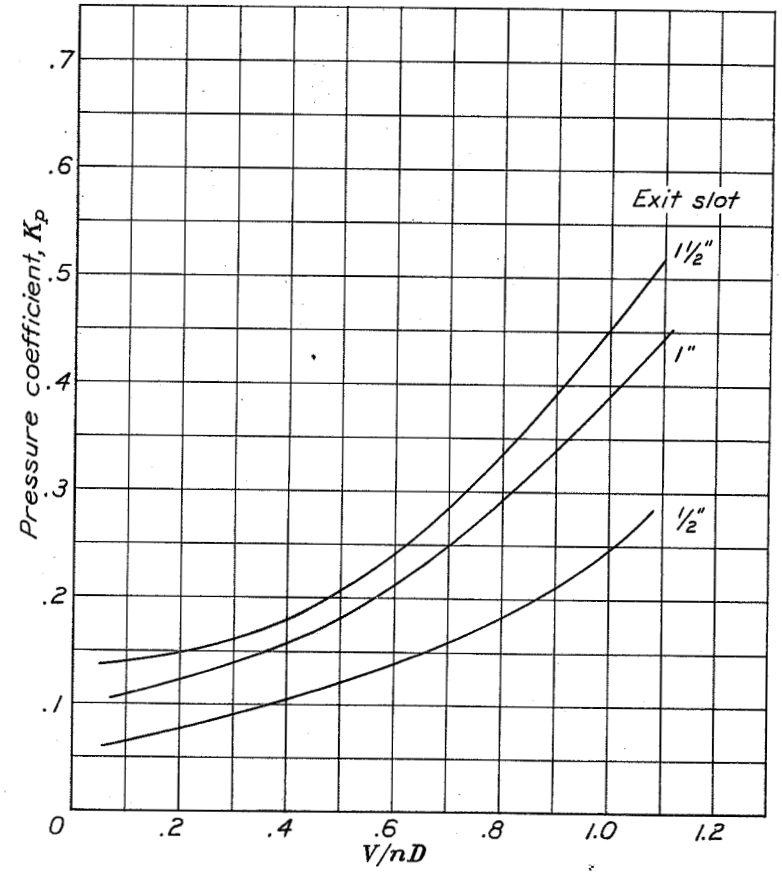

Figure 21.

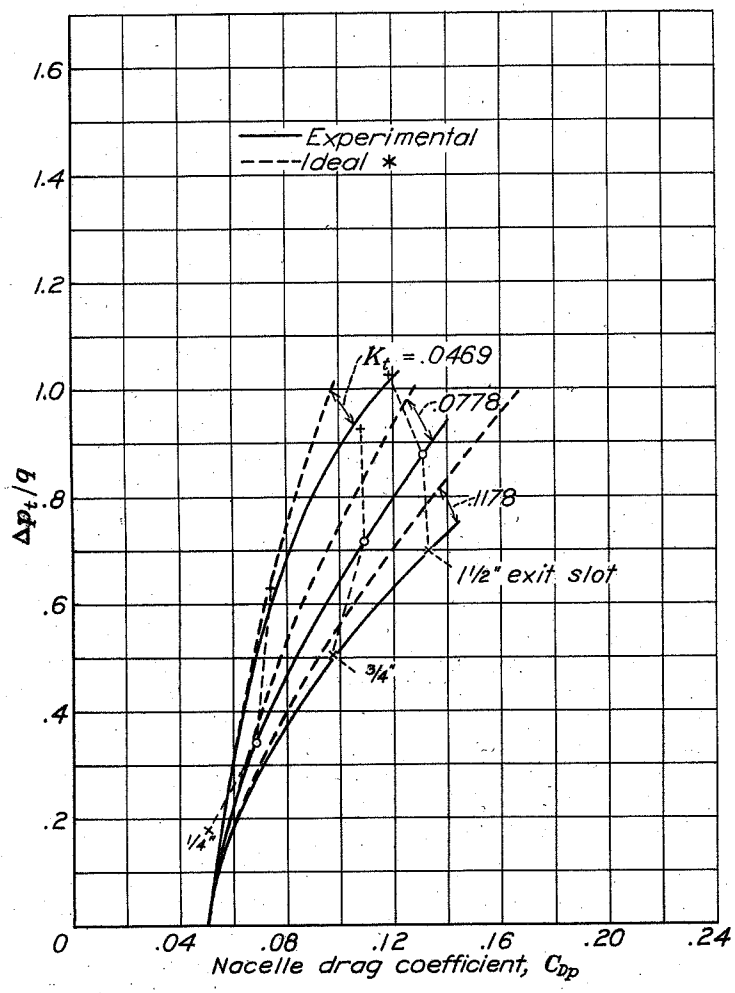

Figure 22.

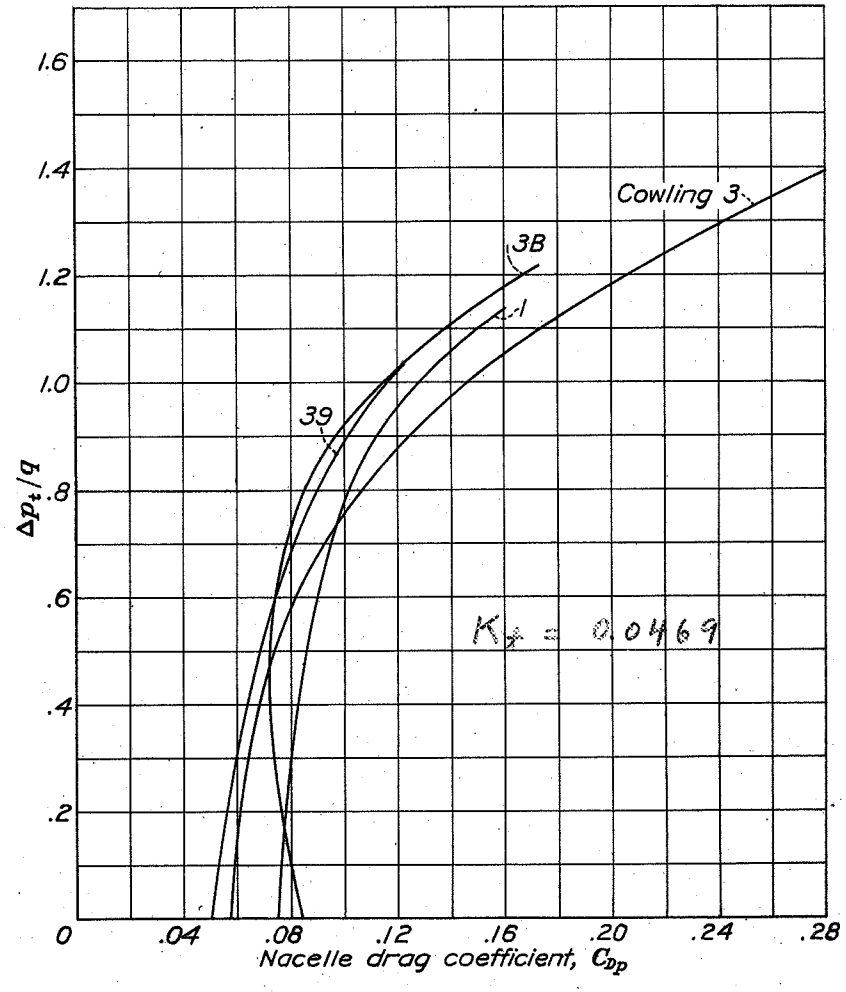

Figure 23.

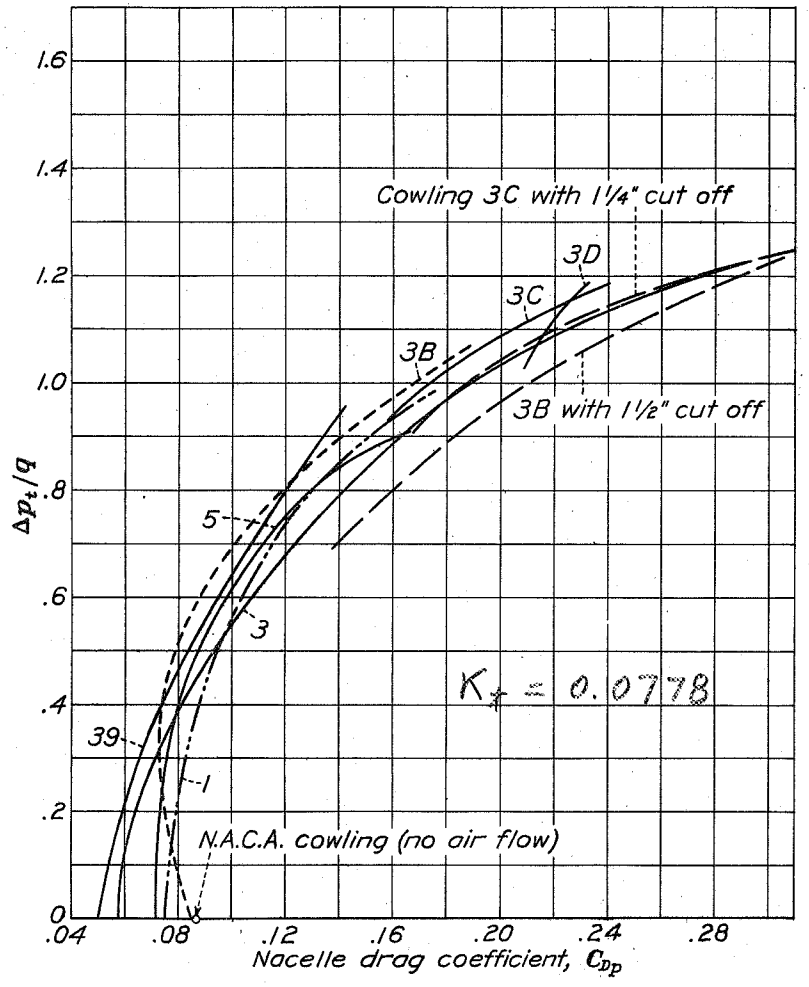

Figure 24.

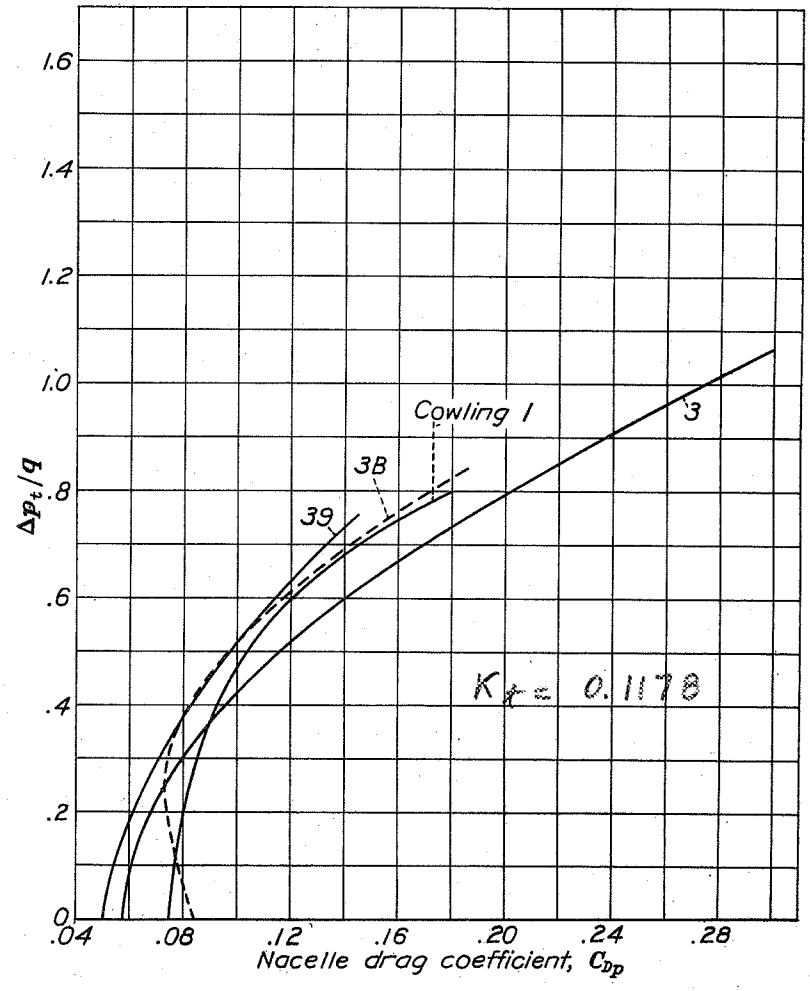

Figure 25.

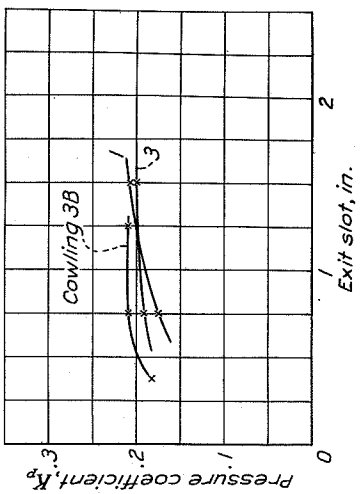

Figure 26.

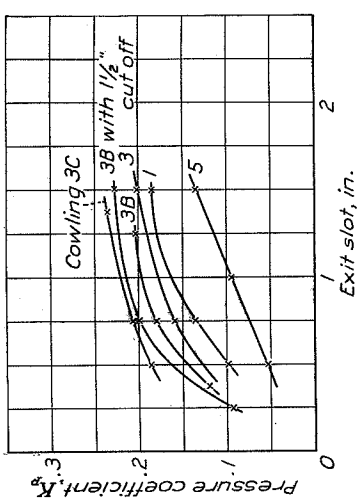

Figure 27.

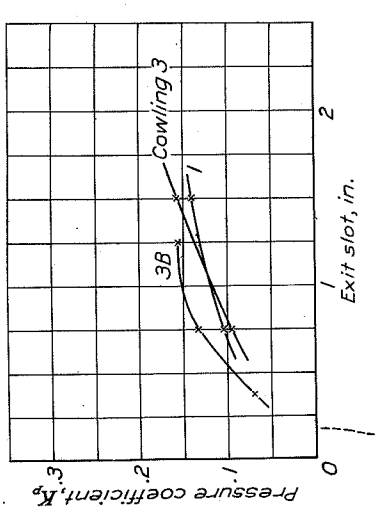

Figure 28.

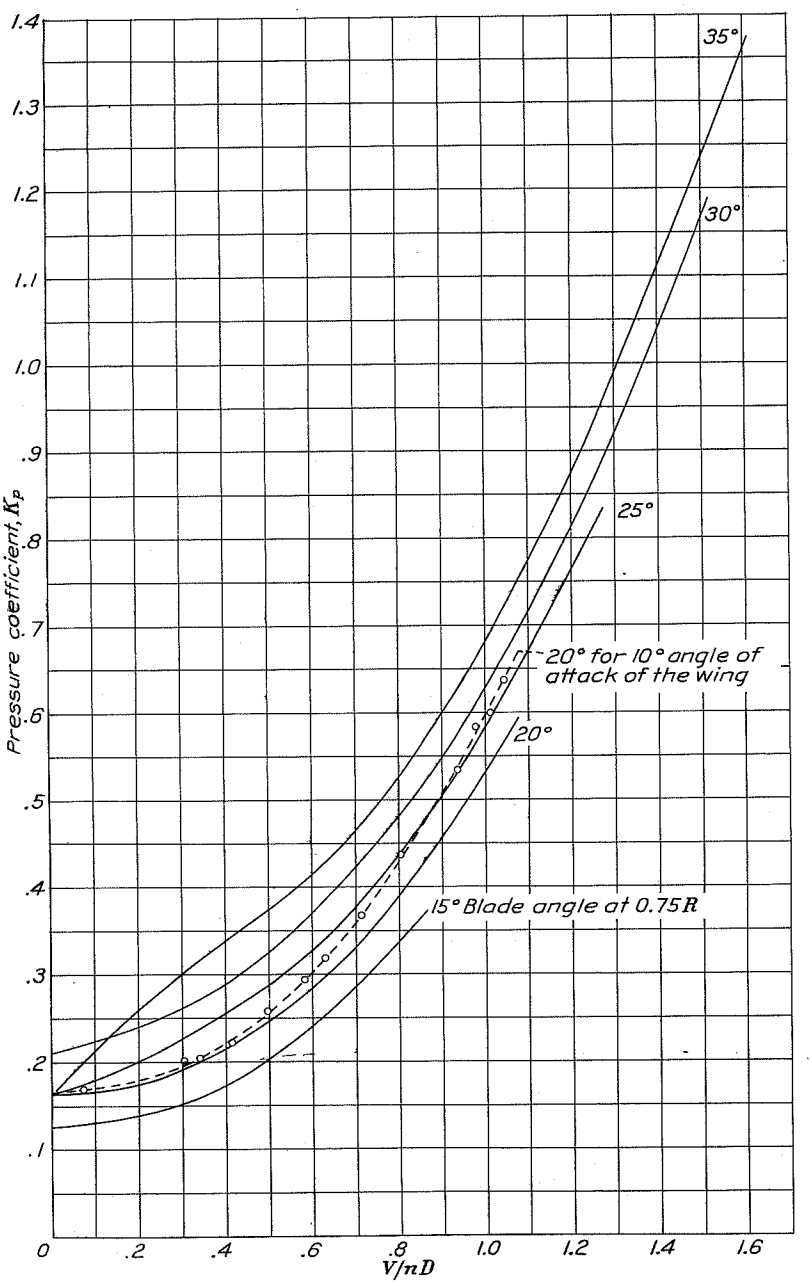

Figure 29.

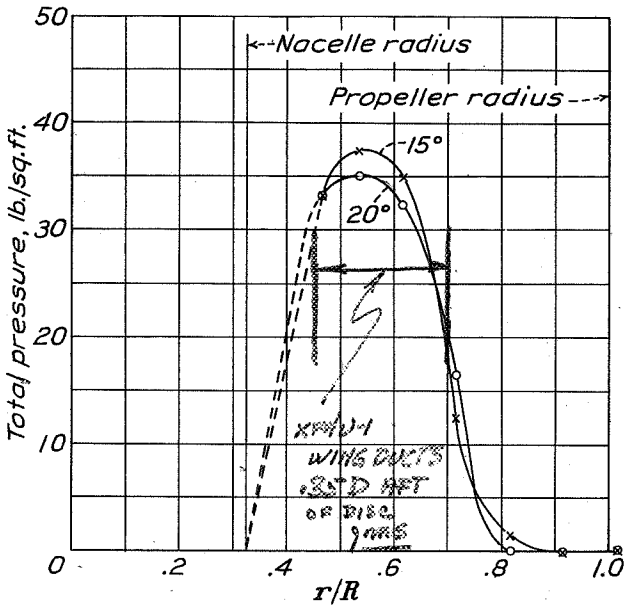

Figure 30.

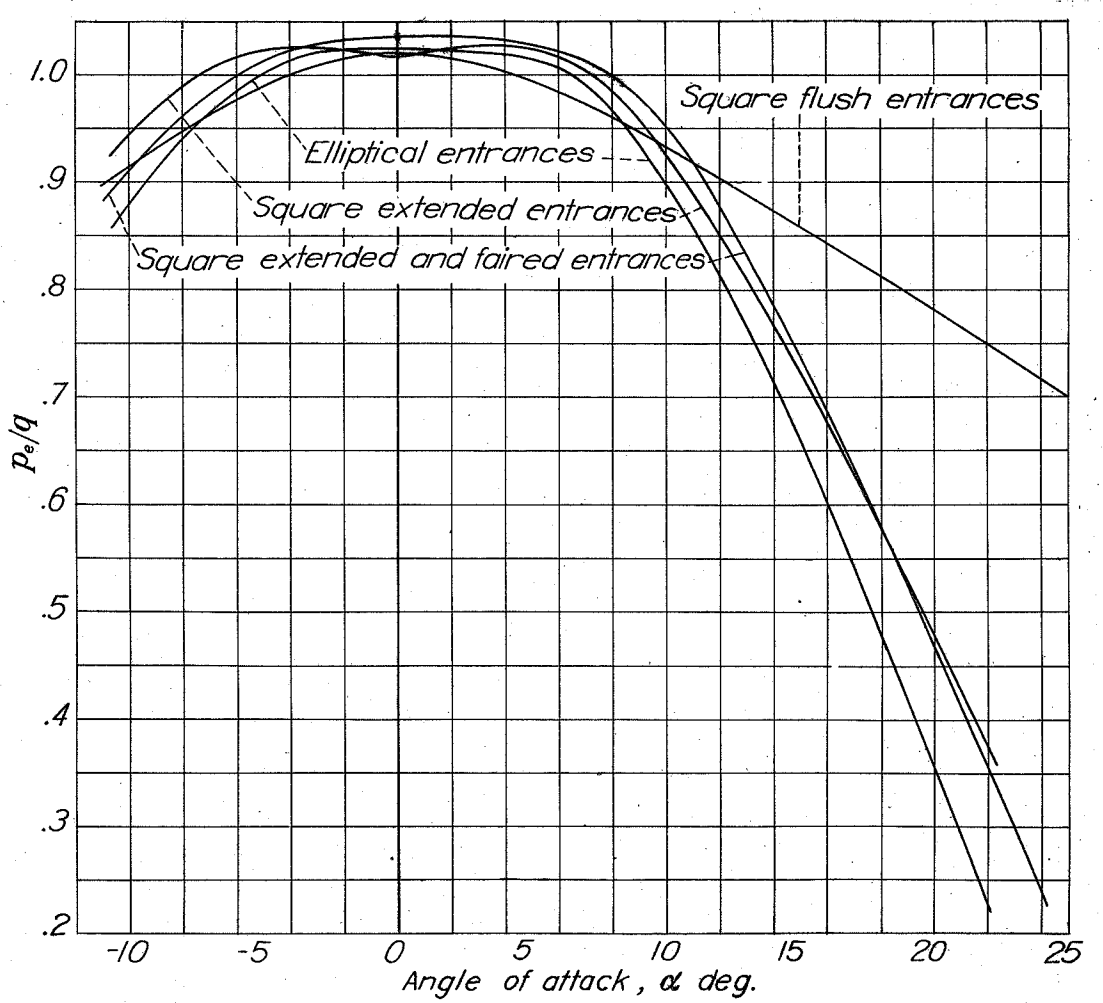

Figure 35.

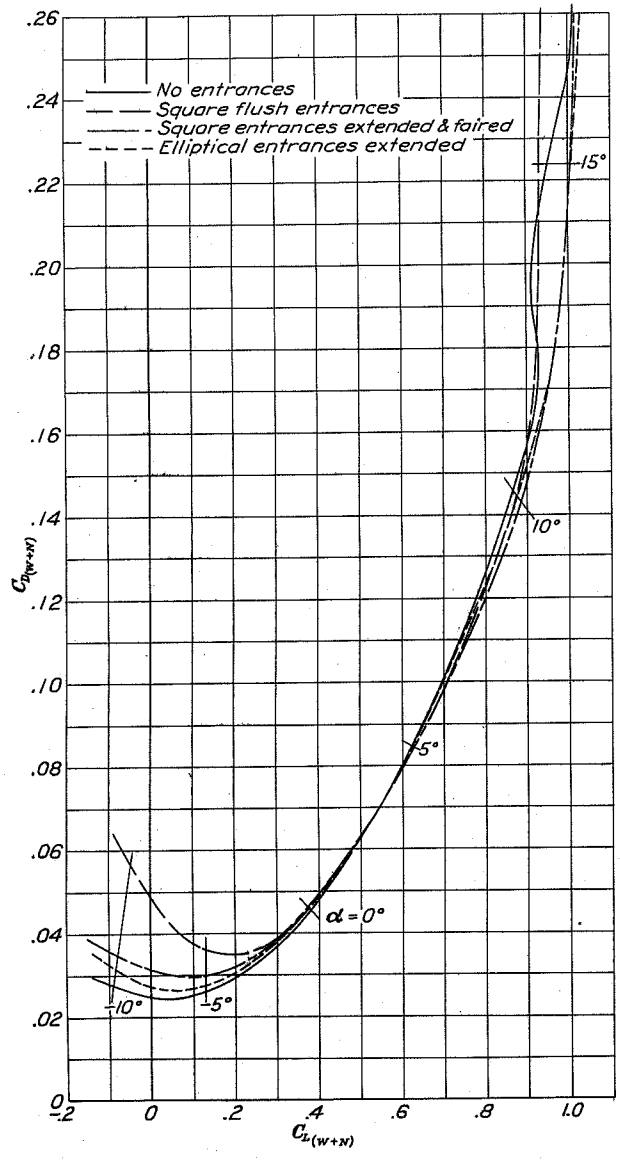

Figure 31.

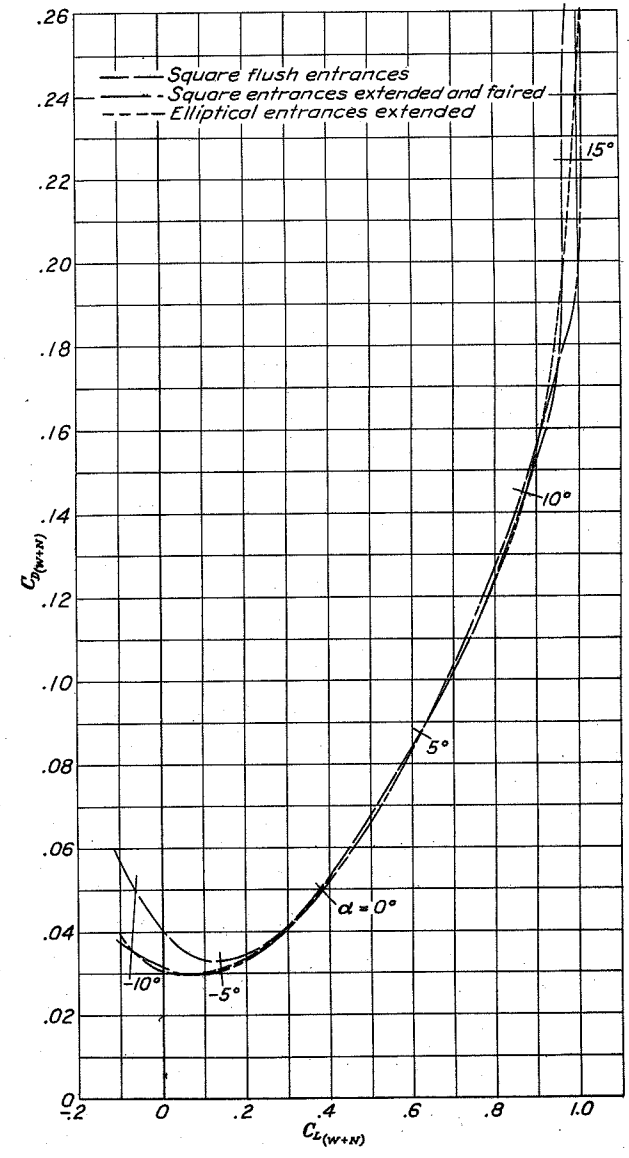

Figure 32.

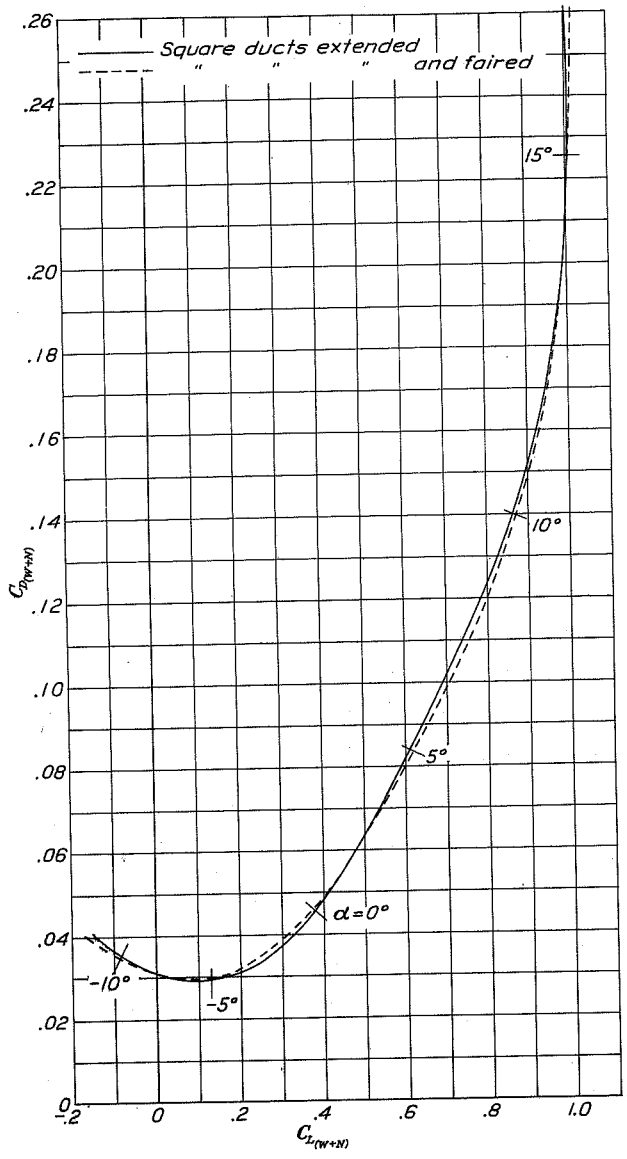

Figure 33.

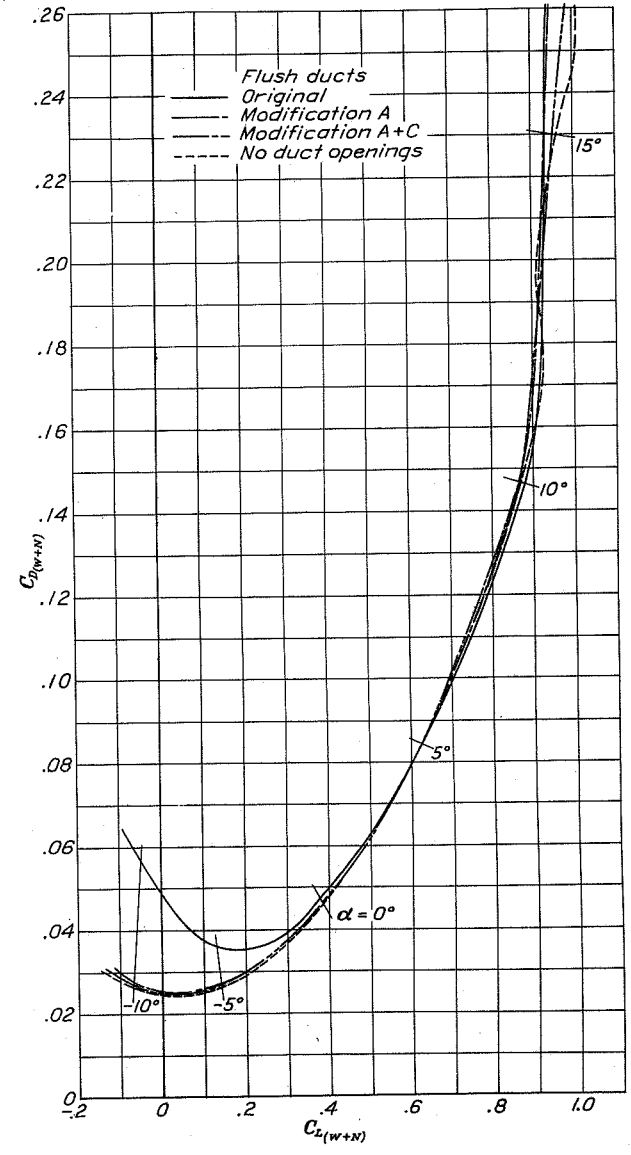

Figure 34.

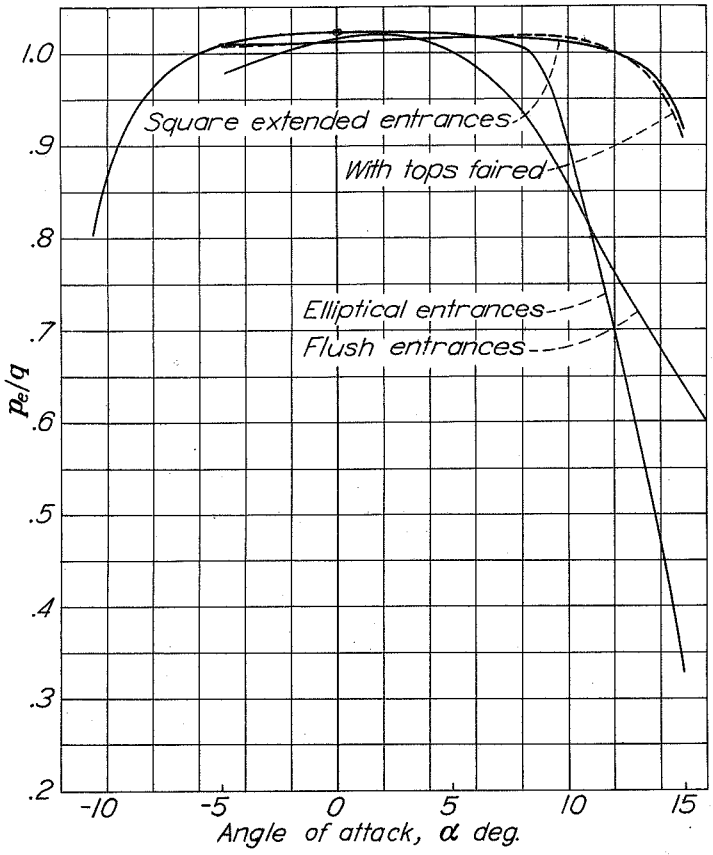

Figure 36.

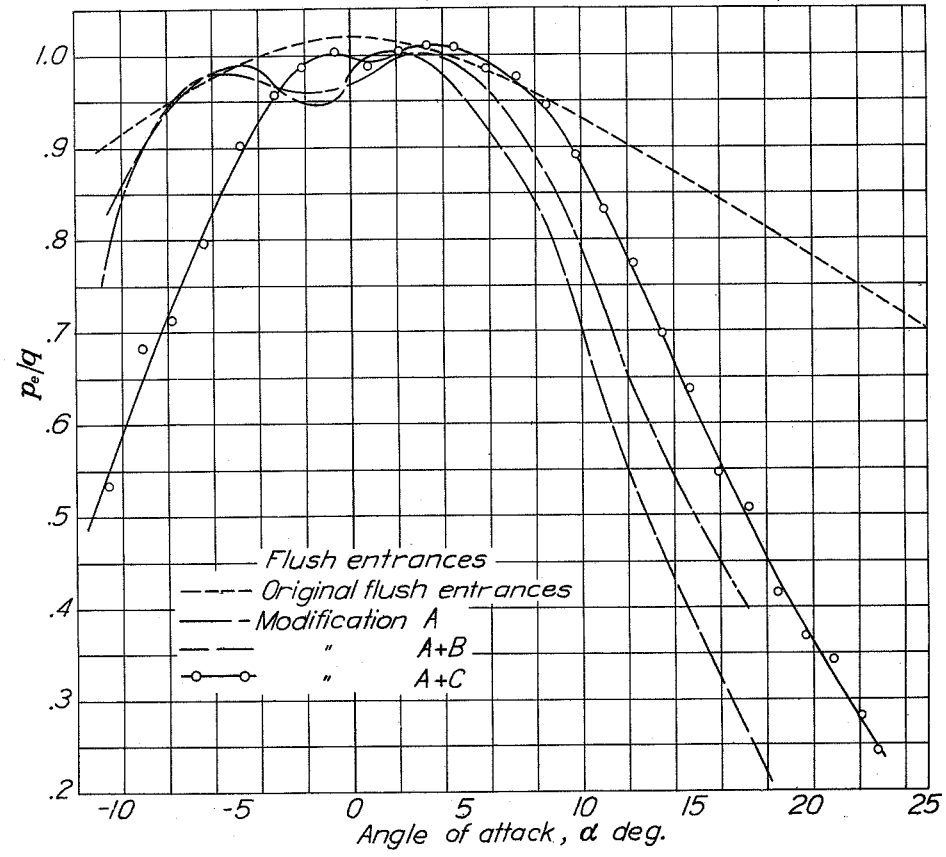

Figure 37.

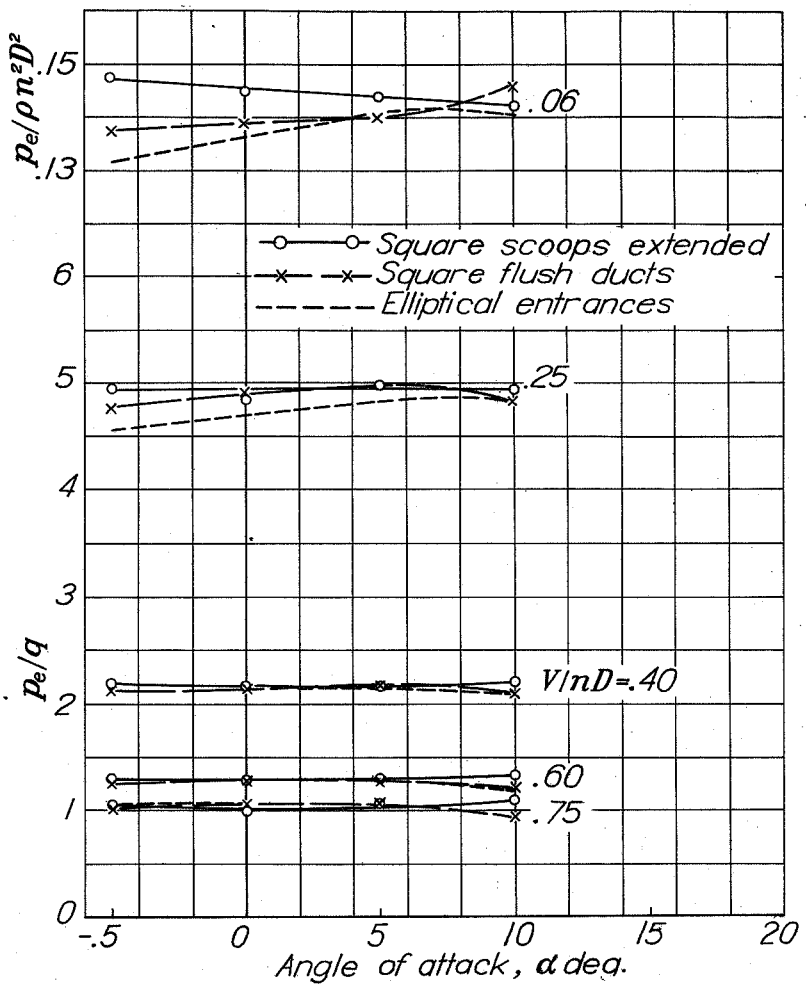

Figure 38

Figure 39.

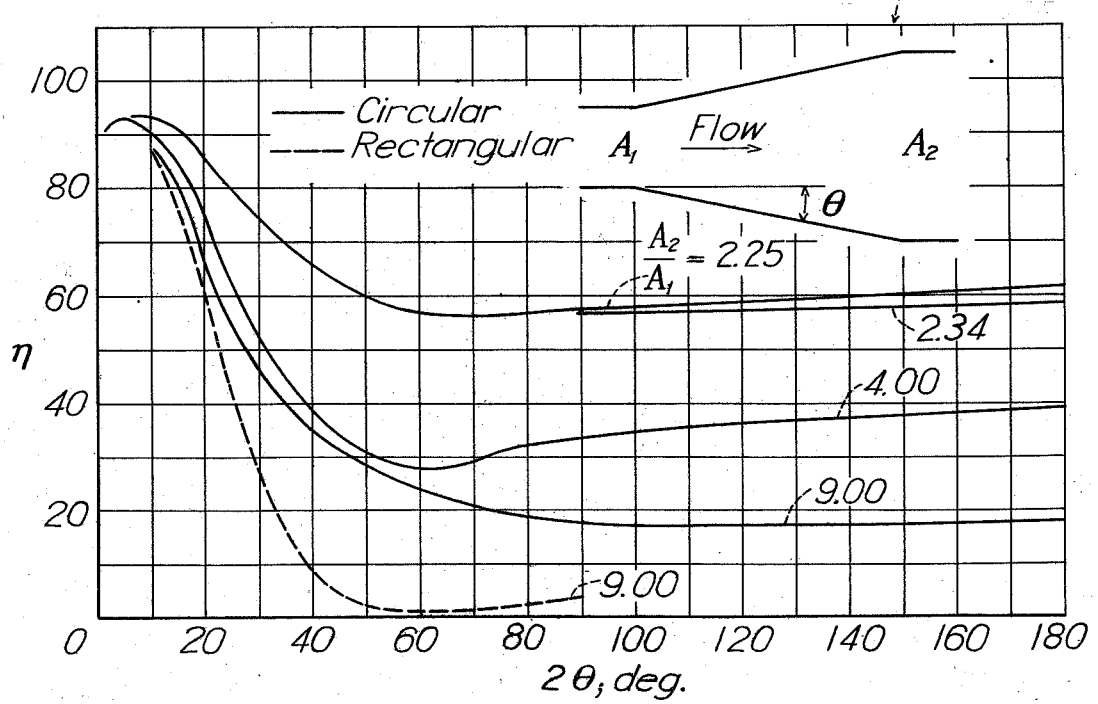

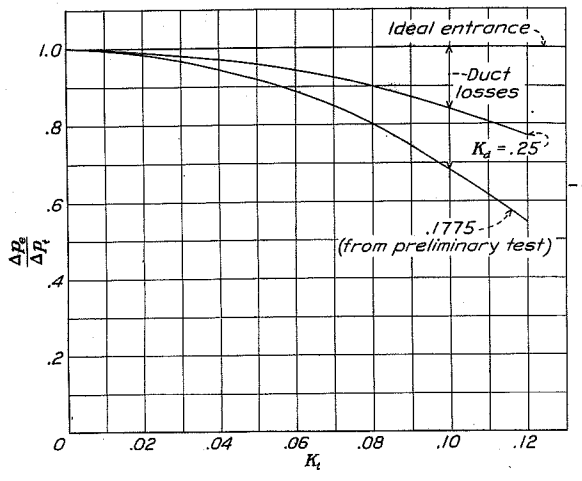

-----Figure 40

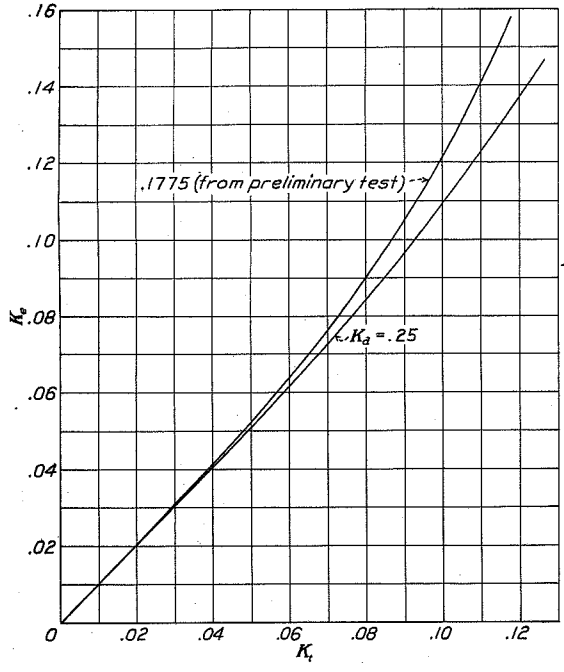

-----Figure 41

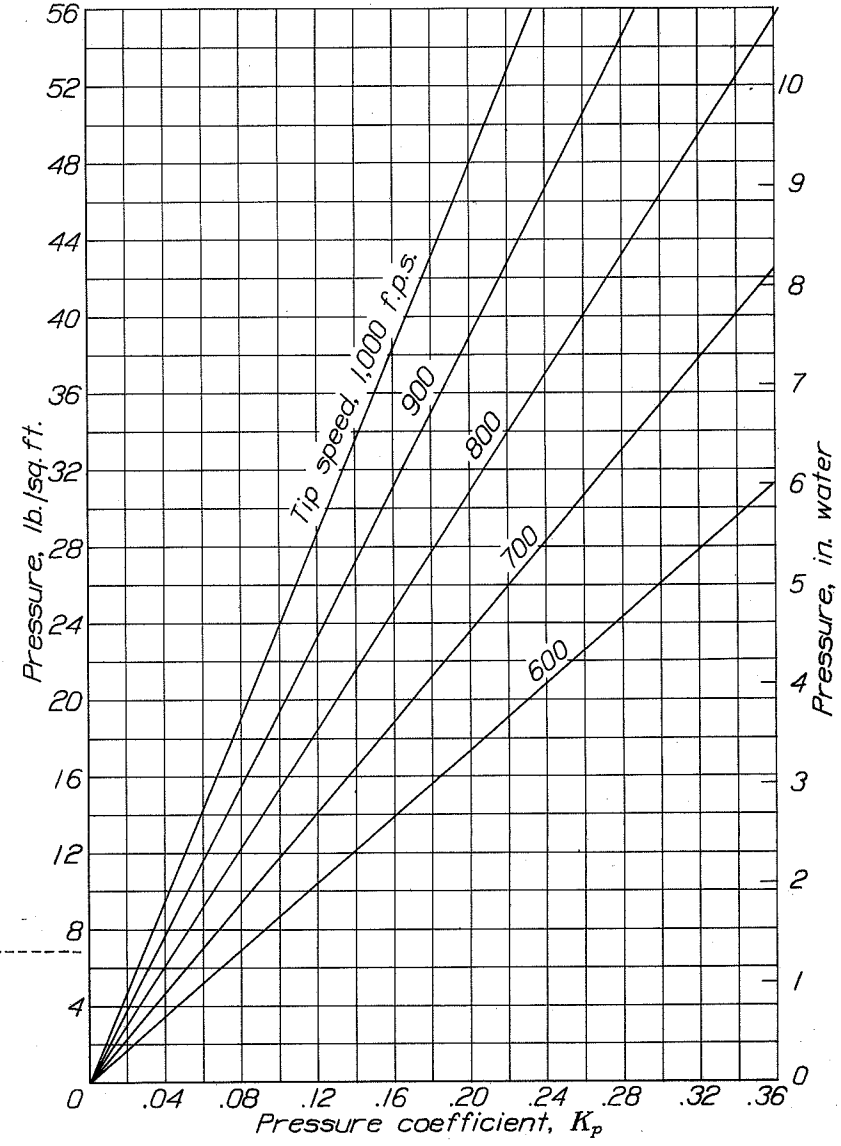

Figure 42-------

Figs. 40, 41, 42